

Aleksei Ponomarenko-Timofeev

UPLINK TRANSMISSION CONTROL METHODS IN LSA-ENABLED CELLULAR NETWORKS

Faculty of Information Technology and Communication Sciences
Master of Science thesis
March 2019

ABSTRACT

ALEKSEI PONOMARENKO-TIMOFEEV: Uplink Transmission Control Methods in LSA-Enabled Cellular Networks

Tampere University

Master of Science thesis, 54 pages, 0 Appendix pages

March 2019

Master's Degree Programme in Information Technology

Major: Communication Systems and Networks

Examiners: Asst. Prof. Sergey Andreev, Prof. Yevgeni Koucheryavy

Supervisors: Asst. Prof. Sergey Andreev (Tampere University), Dr. Alexander Pyattaev (YL-Verkot Oy), Prof. Yevgeni Koucheryavy (Tampere University)

Keywords: LTE, LSA, Dynamic, Interference, Control, Airport

As of now, multiple approaches to increasing network throughput are being studied. For instance, mmWave communications are expected to deliver increase in network throughput to 7 Gbps over 60 and 28 GHz. As a consequence of increasing frequency, the range of communication decreases, but new possibilities arise, such as directional transmissions. Another approach is offloading traffic onto neighbors in case they are connected to a faster link. In case of mobile devices it leads to decreased battery lifetime and increase of power consumption. Another approach is reusing stale bands that were reserved for services that are obsolete and/or defunct. However, there are cases when stale bands are allocated to services that are not defunct, but their activity is low. In this case, it is impossible to reallocate the bands. Despite that, it is still possible to use these bands by using LSA approach by sharing bands between the original owner (incumbent) and licensee. Licensee will need to satisfy the terms of the licensed sharing by keeping the interference power below the threshold and vacating the bands when latter are requested by incumbent. Hence, we must not use shared bands for delay-sensitive traffic or mission-critical services. One possible application of LTE LSA is non-critical IoT devices that are linked to the power grid (weather stations). Therefore, we should balance between satisfying license agreement terms and keeping the network operational. We also need to realize that LSA approach can be applied in cases when location of the incumbent changes rapidly. In this work, power control methods developed for LSA-enabled cellular networks are given. These methods were built for dynamic LSA scenarios, when position of the incumbent changes rapidly and licensee has to readjust power limits on the infrastructure. Aside from that, some minor improvements that were done to the algorithms are described, as well as practical operation example is shown.

PREFACE

Simulation parts of the study were performed in the Faculty of Computing and Electrical Engineering in TUT. Live trial was performed at Brno University of Technology (BUT) in Czech Republic. I would like to thank Prof. Yevgeni Koucheryavy, Prof. Samoylov Konstantin, Prof. Jiří Hošek, Asst. Prof. Sergey Andreev for providing me with opportunity to work in great place and guiding me during the studies. The study would have been impossible to perform without their support.

I would like to thank Dr. Irina Gudkova, Dr. Evgeny Mokrov for support, constructive criticism and patience while giving clear explanations of analytic methods used for estimating network performance. I do hope that we will keep communicating.

Furthermore, I would like to thank Dr. Alexander Pyattaev for teaching me how to use the SLS, introducing me to Gentoo distribution and giving me an opportunity to work on projects that I am interested in. And what is very important, thanks for teaching me to ask the question “Why?” during studies, because causality rules the world and helps us to solve a number of problems.

I would also like to thank Pavel Boronin and Mariia Komar for supporting me during interesting times when everything was uncertain. I hope that after all perturbations we will still be able to keep in touch.

Definitely, I would like to thank all of my colleagues, who helped and gave me numerous helpful ideas during the studies. It was a very pleasant period, when we tried to solve problems, had awesome discussions in work and non-work time.

I would also like to thank Prof. Andrey Turlikov for paving the foundation of knowledge and basic skills that I currently stand on. Also for assisting me in my previous studies, and encouraging healthy practices for cross-validating the results.

I am also thankful to my girlfriend Olga Ledovskaia for supporting me, helping me to switch to different types of tasks when studies almost entered a halted state.

I would also like to thank the Gentoo and ArchLinux community for writing great Wiki, that helped me configure cluster computing environment that drastically accelerated the simulations and was beneficial for my colleagues.

This thesis is dedicated to my parents, Elena and Alexey Ponomarenko, who supported me even in the most boldest moves, cheered me up and gave me everything to be whoever I want to be.

Tampere, 2019.02.21

Aleksei Ponomarenko-Timofeev

CONTENTS

1. Introduction	2
1.1 Mobile traffic growth and state-of-art solutions	2
1.2 Problem definition	7
1.3 Thesis outline	7
2. LSA Architecture Principles	9
2.1 LSA entities and their functions	9
2.2 Relations between LSA entities	11
3. System level simulations of LSA-enabled cellular networks	15
3.1 Evaluated scenario	15
3.2 Simulation toolkit description	19
3.3 Verification and analytical results	21
4. Uplink transmission control methods	25
4.1 Implemented control methods	25
4.2 Power control evaluation	31
4.3 Algorithm performance evaluation	33
5. Practical operation of LSA-enabled cellular systems	37
5.1 Deployment and equipment	37
5.2 Measurement results	43
6. Conclusions	48
Bibliography	50

LIST OF FIGURES

1.1	Mobile traffic forecasts and statistics, derived from [1, 2]	3
1.2	MIMO and MU-MIMO system examples	5
2.1	Registration procedure flowchart	12
2.2	Administrative structure of LSA System	14
3.1	Administrative composition of the scenario	16
3.2	Proposed simulation scenario	17
3.3	General structure of the simulator	20
3.4	Single-cell, single-band LSA model	22
3.5	Single-cell, two-band LSA model	23
3.6	UL TX power minimum in simulation and analytic model	24
4.1	UL TX power at 5 seconds	29
4.2	UL TX power at 15 seconds	30
4.3	UL TX power at 20 seconds	31
4.4	Average UL TX power limit	32
4.5	Interference received by an airplane	33
4.6	Dynamic stepping curve	34
4.7	Number of steps taken to reach satisfactory conditions	35
5.1	Operational diagram of client application	39
5.2	Operational diagram of server application	41
5.3	Deployment of the trial (Adapted from [3])	42

5.4	Configured UL TX power limits for SHANNON	44
5.5	Measured interference at cart for SHANNON	45
5.6	Configured UL TX power limits for SMART LIMIT	46
5.7	Measured interference at cart for SMART LIMIT	46

LIST OF TABLES

5.1 Parameters of the BUT LTE network	37
---	----

LIST OF PROGRAMS

4.1	LIMIT_POWER algorithm	26
4.2	SHANNON algorithm	27

LIST OF ABBREVIATIONS AND SYMBOLS

ACK	Acknowledgment
ATC	Air Traffic Controller
API	Application Programming Interface
BS	Base Station
BUT	Brno University of Technology
CSI	Channel State Information
DL	Downlink
DSP	Digital Signal Processing
MFCN	Mobile/Fixed Communication Network
MIMO	Multiple Input Multiple Output
D2D	Device to Device
WiFi	Wireless Fidelity
FSPL	Free Space Path Loss
LC	Licensed Shared Access Controller
LOS	Line Of Sight
LR	Licensed Shared Access Repository
LSA	Licensed Shared Access
LSRAI	Licensed Shared Access Radio Resource Availability Information
LTE	Long Term Evolution
MC	Monte Carlo
MCS	Modulation Coding Scheme
MEC	Multi-access Edge Computing
MFCN	Mobile Fixed Communication Network
MU-MIMO	Multi-User Multiple Input Multiple Output
MTC	Machine Type Communications
NLOS	Non Line Of Sight
NRA	National Regulatory Authority
OAM	Operations, Administration and Management
OSPF	Open Shortest Path First
PAA	Phased Antenna Array
RSPG	Radio Spectrum Policy Group
RUDN	Peoples Friendship University of Russia
SAB	Service Area Broadcast
SLS	System Level Simulator
SU-MIMO	Single-User Multiple Input Multiple Output
TUT	Tampere University of Technology

TX	Transmitter
RX	Receiver
UE	User Equipment
UL	Uplink
URL	Uniform Resource Locator
c	Speed of light in a vacuum $\approx 3e8m/s$
C	Channel capacity
B	Channel bandwidth
$SINR$	Signal to interference and noise ratio of the channel
f_c	Carrier frequency
d_{CE}	Distance from the edge of the cell
h_{air}	Airplane altitude
I_{lim}	Interference limit
I_{inc}	Interference at incumbent (measured)
I_{est}	Estimated interference at incumbent
I_{dyn}	Dynamic power reduction steps

1. INTRODUCTION

In this chapter, review of state-of-art approaches to solving the issue of mobile traffic growth is given, as well as their brief description.

1.1 Mobile traffic growth and state-of-art solutions

As multiple forecasts indicate, volume of mobile traffic will have an exponential growth in the near future [2]. These forecasts are given by multiple telecommunication equipment manufacturers such as Ericsson, Cisco and Qualcomm. Growth of volume is caused by both rising demand of applications (live streaming [4], virtual/augmented reality (VR/AR) [5]) and increase in total number of interconnected devices [6]. Moreover, this trend is supported by the fact that in 2016 monthly mobile traffic grew by 63%, increasing from 4.4 exabytes in the end of 2015 to 7.2 exabytes in the end of 2016. Apart from that, over the past 5 years mobile traffic volume increased 18-fold, and average mobile cellular connection rates grew 3-fold, rising from 2.0 Mb/sec to 6.3Mb/sec [1]. Measured volumes of the mobile traffic are also appear to be growing with an increasing rate. Volume growth is stable between 50 and 80 percent each year according to [7]. In absolute units, it means that growth rate is increasing rapidly. Moreover, Cisco released Visual Network Index whitepaper [1], containing estimates of mobile traffic in oncoming years. These predictions can be seen in Figure 1.1 as well as currently measured statistics. It can also be seen that growth of voice traffic is negligible, compared to data traffic. This is explained by the fact, that newer devices, that are being introduced onto the market, generate more traffic per unit. This is caused by both increase in quality of the devices (cameras in smartphones and video quality on broadcasting resources) and introduction of newer services, such as live streaming.

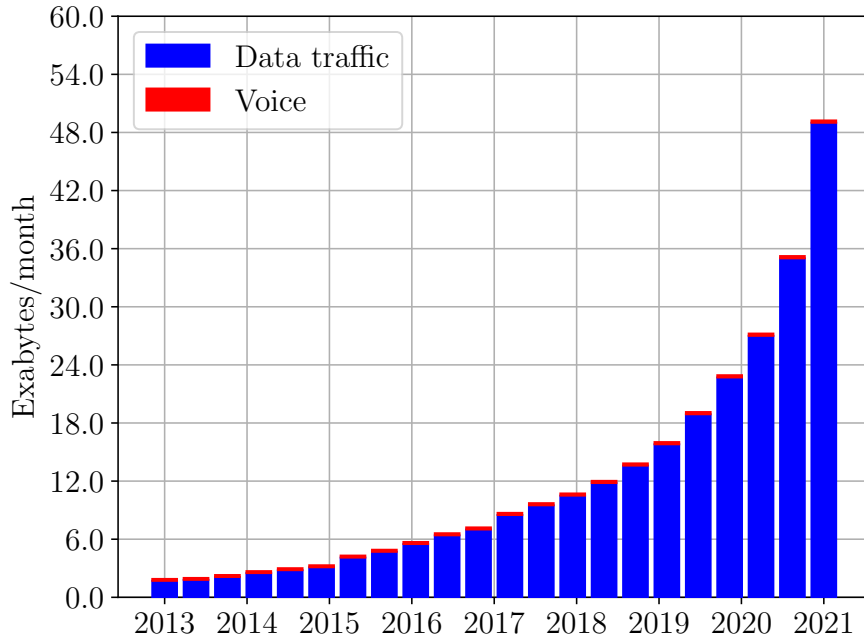


Figure 1.1 Mobile traffic forecasts and statistics, derived from [1, 2]

Modern radio networks will not be able to handle such volumes of traffic and need to be upgraded. Previously, such issues were resolved by “command and control” approach. This approach statically allocates certain frequency bands to specific operator or service (mobile network operators (MNO), radars, television (TV) broadcast) in an exclusive manner. It means that these bands must not be used by anyone other than the licensed owner, even if the bands are not actively used at the moment. This leads to a situation when bands are underloaded and capacity is wasted due to administrative limitation of the system. Therefore, it may be viable to introduce a flexible approach to managing the spectrum. This can be accomplished by employing unlicensed bands, which means that data can be transmitted over bands by anyone who has access to appropriate equipment. This approach has a downside of introducing bands without any quality of service (QoS) guarantees, since operators have equal priority and will interfere with each other. This situation can be observed in 2.4 GHz range of 802.11 wireless networks [8, 9, 10] in densely populated and public places. Moreover, migrating to unlicensed spectrum is also complicated by the fact that accounting systems will need to be redesigned from scratch, complicating the situation even further. Therefore, simply switching to unlicensed spectrum may not be enough to handle the problem. Therefore, in order to address the issue of bandwidth depletion, multiple solutions are being studied, these include, but are not limited to:

- Dense and Ultra-dense networks — solution that is based on decreasing the communication range while increasing link throughput [11, 12]. By decreasing the range and transmit (TX) power, we decrease interference in the network to a certain extent. However, we are unable to limit the coverage, since this parameter is dictated by user. Therefore, more equipment will be needed to serve the same area as before. The most efficient way to increase capacity of the network and therefore throughput is by increasing bandwidth. This can be easily deduced from Shannon-Hartley theorem. Since we decreased transmit power in the system, we also reduced the interference. This is caused by the fact that most of the interference may come from neighboring devices. The signal to interference and noise ratio (SINR) in our system does not change drastically because of this, since it is comprised of both received signal power and interference. If we increase the bandwidth, we will observe almost linear rise in capacity of the channel. Therefore, using bands at 28 and 60 GHz is considered as a solution to the problem. However, if we increase frequency, we also may notice that link quality deteriorates faster than before, if we start increasing the distance between TX and receiver (RX). Moreover, radio-transparency of the objects decreases drastically at these frequencies, compared to current conventional communication systems. However, this can be mitigated with beamforming, which enables directional transmissions and can be achieved with phase antenna arrays (PAA). This way devices can both reduce interference and increase received signal strength on the destination antenna. Beamforming also enables devices to use non-line-of-sight (NLOS) propagation paths (reflections, diffractions and scattering). Moreover, beamforming is also considered as one of tools for improving security of the transmission [13, 14] by simply narrowing a set of locations where eavesdropper can intercept radio signal.
- Multiple input, multiple output (MIMO) — instead of using one receiving and one transmitting antenna for exchanging information, our system utilizes multiple antennas [15, 16]. It is important to note that this approach differs from PAA, since it is not limited to beamforming. This helps us increase link throughput by optimizing transmitted signal in such way that it is more robust in terms countering harmful effects of the radio channel. The transmitter and receiver attempt to estimate channel characteristics prior to sending the data and use these to their advantage. Also, system attempts to improve link throughput by having multiple data streams sent to the UE simultaneously. This approach is already implemented and is an essential component in multiple networks, such as 802.11n, 802.11ac and long term evolution (LTE). Furthermore, multiuser MIMO (MU-MIMO) can further help increase throughput

by being able to handle data streams from multiple users simultaneously [17].

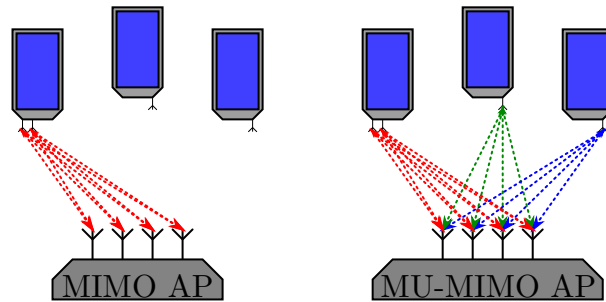


Figure 1.2 MIMO and MU-MIMO system examples

However, this approach requires introduction of complex digital signal processing (DSP) techniques in order to process channel state information (CSI) and fine-tune the signals. Therefore, it may not fit applications that are constrained in terms of power consumption and complexity.

- Drone cell — an approach which is focused on rapidly providing extra capacity where it is needed [18, 19]. While being similar to a solution with mobile base station (BS) van, it has a benefit of being faster and cheaper [20]. While it is obvious why this approach deploys faster than a van with mobile BS, it must be noted that there are a few incentives that are important to the operator of the network. A van must be driven by a human and communications engineer is needed to set up the mobile BS. However, drone requires at most only one operator and is not bound to any transport infrastructure. It assumed that drone will be capable of receiving flight mission and acting autonomously. Network engineer can also be located in a control center and configure settings relevant to mobile fixed communication network (MFCN) remotely. Therefore, if multiple drone cells are deployed, it may be possible for one network engineer to configure them. Apart from that, drone cells can be used in case infrastructure of the operator has failed completely and emergency backup is needed due to natural disaster. This is caused by the fact that drone is in the air (it may be built as a quad-copter, small zeppelin or a plane) and is capable of maintaining its position. From all of above it can be noted that this approach is similar to densification of the network, however it is aimed at handling critical situations when additional throughput is required.
- Device-to-device (D2D) offloading — based on assumption that links can be established through third-party user equipment (UE) [21, 22]. As an example we may consider case when UE1 is out of BS coverage, but his neighbor UE2 successfully established link with BS and announced it via WiFi network. If

UE1 receives this announcement, it can connect to UE2 and route the data it wants to transmit via UE2. However, this approach is not strictly limited to WiFi announcements. Also, in order to stimulate forwarding of the data, certain incentives must be provided to users of the UEs, since this solution causes extra strain on the battery and may not be acceptable for every user [23].

Apart from the mentioned solutions there is also an approach called licensed shared access (LSA) [24, 25]. It is based on a fact that there are numerous frequency bands that are used by services that are operating within short periods. These bands are underutilized, but at the same time they cannot be reallocated for use in newer systems. This can be caused by the fact they are used by services that are active and cannot be terminated. On the other hand, it is still possible to enable sharing if harmful interference is avoided or kept to a minimum. In other words, LSA enables sharing otherwise statically allocated bands between two parties under certain license conditions [26]. In terms of frequency band management it lies between “command and control” mechanism and unlicensed spectrum, since it is possible for third party to use licensed bands, but certain conditions apply. It helps us use frequencies that are underutilized but cannot be reallocated. Since the service depends on whether original owner of the bands (incumbent) is using them, the service is not reliable and can deteriorate at random time instances. This makes LSA unsuitable for delay-sensitive services that are intolerable to loss of data. However, LSA approach can still be used for non-critical machine to machine communications (MTC) applications [27]. Multiple LSA trials were performed in Europe as of now, some of them are listed below:

- LSA/ASA trial in Finland, Ylivieska — Live trial, which aimed at demonstrating feasibility of LSA/ASA concept in terms of increasing network capacity and protecting incumbent [28, 29]. Trial covered both evacuation and activation procedures for the LSA/ASA bands. Role of incumbent in this trial was taken by a news crew with a mobile camera, that initially used 2.4 GHz for service area broadcast (SAB) [30]. During that trial service on shared band was simply terminated when incumbent needed to use the bands.
- Dynamic LSA trial in Czech Republic, Brno — trial aimed at studying how operator can refrain from termination of the service on shared bands while adhering to the LSA license terms [31]. The trial was performed on one of the floors of Brno University of Technology (BUT) with one incumbent entity and multiple UE devices. Main objective of the trial was to study how dynamic management policies can be integrated into the system, and study their performance in terms of incumbent interference and throughput on shared bands.

- LSA trial in Spain, Barcelona — demonstration of a functioning LSA-enabled system sharing frequency bands between programme-making and special event (PMSE) services and MFCN [32]. Demonstration was built upon study on coexistence of MFCN and PMSE performed by SETSI. LSA infrastructure in this trial was built according to [33]. However MFCN was simulated and primarily comprised of macro and small cells, propagation characteristics for the deployment were based on Spanish radio environment map.

Unfortunately, the LSA-enabled system still depends on actions of the incumbent, which means that expected QoS is lower than in conventional systems. It is possible to limit the effects of incumbent presence in case license conditions are built around limiting harmful interference to incumbents services.

1.2 Problem definition

As it was noted, in case license conditions are built around interference management, it is possible to take multiple paths towards simultaneously satisfying LSA license conditions and maintaining system operation. While primitive solutions such as temporarily disabling service in the area, where incumbent is active, is a solution, it is far from optimal. Therefore, there is a need to study, whether there are any other solutions to the problem. If there are, it is important to evaluate how each of the solutions perform and whether it may be possible to implement in the networks.

1.3 Thesis outline

In this thesis multiple methods of reducing the interference towards incumbent are given. Apart from that, possible opportunities to decrease the impact of incumbent activity will be given, as well as an evaluation of how methods perform in dynamic scenario. The scenario will assume that license conditions are built only around limiting harmful interference. Therefore, uplink (UL) TX control methods will also be based on managing the transmit power of the UE devices. Thesis is therefore structured in a following manner:

- Section 2.1 defines entities, that are essential in LSA-enabled communication systems. Furthermore, core functions, required for operation of LSA-enabled system, are described in this section. After entities and their functionality is defined, possible interactions between entities are defined in section 2.2. Interactions are defined from technical and business standpoints.

- Section 3.1 describes scenario used for simulation of LSA-enabled system. Simulation toolkit, that was used for obtaining the result presented in the thesis, is described in section 3.2. Further, analytic models used for estimation of LSA-enabled system performance in various cases and calibration results are covered in section 3.3.
- Sections 4.1 and 4.2 is dedicated to describing implemented and studied up-link control methods, providing plots that demonstrate how UL TX power is changed throughout the simulation. Code listings in Python are also provided to assist it this task. Section 4.3 focuses on the optimization of one of the methods, demonstrating the benefit of picking non-fixed step.
- Section 5.1 describes equipment and deployment that were used in live testing campaign in Brno, while 5.2 contains results of latter measurements and conclusions based on them.

2. LSA ARCHITECTURE PRINCIPLES

In this section, entities and relations of LSA-enabled system are demonstrated. It is important to note, that we will review the structure from both technical and administrative standpoints.

2.1 LSA entities and their functions

In order to make further explanations clear and understandable, we need to study how conventional LSA system is built. LSA system consists of the four key entities, according to [34]:

- LSA controller (LC) — an entity that is located inside the LSA licensee domain and is capable of connecting to LSA repository. This entity allows licensee to obtain information about LSA band availability from the LR. Moreover, LC can interact with MFCN of the operator in order to map information from the LR to the actual network. It is also used to provide acknowledgments to the LR after required actions have been applied to the MFCN.
- LSA repository (LR) — an entity that acts as a database (DB) that stores information about bands that are available for sharing, as well as protection information and license conditions that apply to certain bands. It can send commands to LCs if needed and receive acknowledgments regarding applied changes. Apart from that, LR allows NRA to monitor the operation of the LSA infrastructure as whole. This entity is also partially responsible for verifying that the system operates within the conditions of the license.
- National Regulatory Authority (NRA) — responsible for keeping track of allocated frequency bands and managing the frequency plan for specific country/region. Acts as a dealer between licensee and incumbent, and resolves discrepancies between the actual radio resource availability and information that is present in the LR.

- Incumbent - original owner of the bands. This party is provided with bands that are underutilized and are available for sharing most of the time. Incumbent is also capable of sharing the bands via LSA system, meaning that no special restrictions are applied to it. Shared bands should be available most of the time, otherwise it may be unfeasible for licensee to use the bands.

These entities must be capable of performing certain functions in the LSA architecture. These functions are essential for operation of the system and interaction with external entities.

Information entry function is needed for input and further use of the information required for correct functioning of LSA infrastructure. This information may be related to set of sharing rules or conditions for specific band between parties. This function also allows storage of multiple other data structures, such as information on spectrum that can be made available for sharing as well as technical and operational parameters. Sharing license information for each incumbent and licensee with technical and operational specifications as well as protection requirements and spectrum usage conditions for incumbent require this function for storage. As a consequence, this storage function also allows system to keep record of incumbents and licensees identifiers.

Apart from being able to store the data, system must be capable of processing the data to determine whether certain spectrum resources are available for specific licensee. This task is expressed as information processing function, which allows the system to make decisions based on currently available information.

Furthermore, since system is operating with real hardware, it must be capable of configuring the equipment it is linked to. In other words, it must be capable of applying calculated limits and/or availability of shared bands to the network of the licensee. This function is of paramount importance for LC, since it must be able to adjust parameters of the MFCN to satisfy license requirements. Therefore mapping function is also introduced to the system.

The system must also be able to provide logs regarding LSA system status to the NRA, incumbent or licensee. These logs can either be provided on demand or based on a schedule defined by the operator of the system. This functionality is of paramount importance in case diagnostics are required or there is a suspicion that LSA license violation occurred. In European Telecommunication Standards Institute (ETSI) documentation this functionality is referred as reporting function.

Since LSA assumes operation of numerous entities in cooperative fashion, it is im-

portant that communication between them is possible. This functionality is not limited to current state information, but also includes ability to transfer internal LSA commands and parameters between entities. This includes, but not limited to, spectrum availability information and acknowledgment data. Without this function, operation of the system would be impossible.

Moreover, since multiple entities are involved in system operation, there must be support for authenticating messages and providing secure channel for communication. In order to provide this functionality, a set of functions that are responsible for authenticating users and messages is introduced. Moreover, system must support access control to protect confidential user information and prevent malicious parties from accessing it.

However, malicious parties may not only attempt to eavesdrop or illegally obtain the information, but also cause severe overload or degraded performance of the system. Since incumbent may have a rapidly changing requirements for shared bands, resilience towards malfunctions and capability to maintain reliable operation are required. Mechanisms responsible for satisfying these demands are included into sustainability function.

In addition, if security breach or severe performance loss occurred, system must be capable of recovering or applying contingency strategy to minimize the damage. Therefore, capability of detecting discrepancies in the operation of the system is required by ETSI. After system detects certain issues, it must immediately generate status report for NRA, incumbent and licensee.

When all of these functions are in place and operate accordingly, system will be capable of providing a clear and convenient interface for accessing frequency bands shared by the incumbent.

Before continuing, it is important to note that in this study NRA will not be mentioned, since we will assume that incumbent already made the bands available for use in LSA-enabled LTE networks. Moreover, NRA is mostly perceived as maintainer of the LSA infrastructure and does not directly access MFCNs. Therefore, main focus will be on functional aspect of the system, meaning that most of study will be concentrated in areas between incumbent, licensee and licensees MFCN.

2.2 Relations between LSA entities

After entities and requirements for support of various activities in the LSA System are defined, we should also define some of the relations and procedures required for

correct operation of the system, as well as possible outcomes of these procedures.

When a new LC appears in the system, it must first connect to LR and undergo LSA registration procedure. Before this procedure is complete, LC is unable to receive or request any information from LR regarding spectrum availability or make adjustments to LSA-enabled infrastructure. Flowchart of this procedure is given in Figure 2.1.

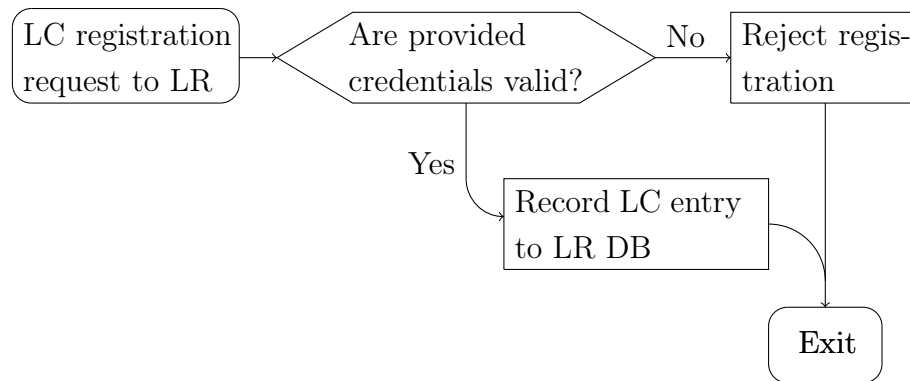


Figure 2.1 Registration procedure flowchart

If LC wants to terminate communications and leave LSA system, it must complete deregistration procedure. After the deregistration procedure is complete, all connections to the LR can be closed. Also, after LC disconnected from LR, bands are no longer operational in MFCN controlled by the LC. In terms of event occurrence, this action is similar to registration, except that deregistration request is sent and LC entry is removed from the LR database.

In case there is a need for LC to obtain latest available information about radio resource availability, it sends LSA radio resource availability information (LSRAI) request to the LR. Authentication credentials are sent along with the request. Request can be simply a database query for LR database. After receiving the request, LR verifies that provided credentials are valid and processes the request. Further, if authentication succeeded, LR compiles a response and sends it to the LC. Otherwise, no response is provided and authentication failure message is provided instead. Finally, when LC receives request response, it can update MFCN settings appropriately.

In certain cases, though, critical updates can appear on LR side, making LC-driven polling with LSRAI request unacceptable. In this case, LR pushes important updates to the LC via LSRAI notifications. As in previous cases, credentials are sent along with the data, in this case, however, LR credentials are used to prevent mali-

cious parties from injecting invalid data into the system. To initiate the procedure, LR compiles the notification, including urgency of the notification and parameters that must be adjusted. Package is then sent to the LC, which verifies credentials and queues the update procedures. Immediately after that, LC responds with an acknowledgement (ACK) to the LR, indicating reception of the notification.

However, since only reception is reported to LR, need for confirmation of successful application of updates is needed. This requirement is satisfied with introduction of LSRAI confirmation, which is used by LC to tell LR that changes from notification were applied. Confirmation is formed by LC after changes are applied to the MFCN and sent with authentication credentials of the LC. After reception, LR authenticates the confirmation and records that changes were applied by specific LC. Upon reception and validation of the confirmation, LR responds to the LC with ACK.

Apart from relations of entities in the system, financial and resource-related relations in this system can be considered as well. Since the incumbent may not share the bands without any incentive, it is assumed that financial incentive will be the main stimuli for participation in the system. Financial resources will originate from the licensee, who will “rent” shared bands, part of these resources will be forwarded to NRA as an incentive. In turn, licensee will obtain extra radio resources to serve users. It was mentioned, that certain reliability limitations apply to this kind of bands before. This means that incumbent is interested in keeping the bands available to the licensee, since if the bands are extremely unreliable, they become unattractive to licensee. If that happens, incumbent will not only lose current licensee, but there is a risk of losing any further sharing agreements. Meanwhile, NRA is interested in keeping the whole system operational and conflict-free, since it receives benefits from each licensing agreement made in the system. If the system is malfunctioning, neither licensee nor incumbent will be eager to communicate through this system. In the meantime, licensee is interested in satisfying sharing license agreements and serving the users. If licensee violates agreements, he may face penalties from the NRA. If licensee fails to serve the users, they may no longer use the service of the licensee and choose different operator. In terms of relations between administrative entities, system can be described with Figure 2.2.

As it can be seen, the driving incentives for the system are financial gain and radio resources (represented by underutilized shared bands). Incumbent provides radio resources to the licensee, while receiving financial compensation through the NRA. NRA is responsible for maintaining the system and resolving conflicts between incumbent and licensee. Driving incentive for NRA is receiving a part of the monetary flow that is directed from licensee to incumbent. Both incumbent and licensee re-

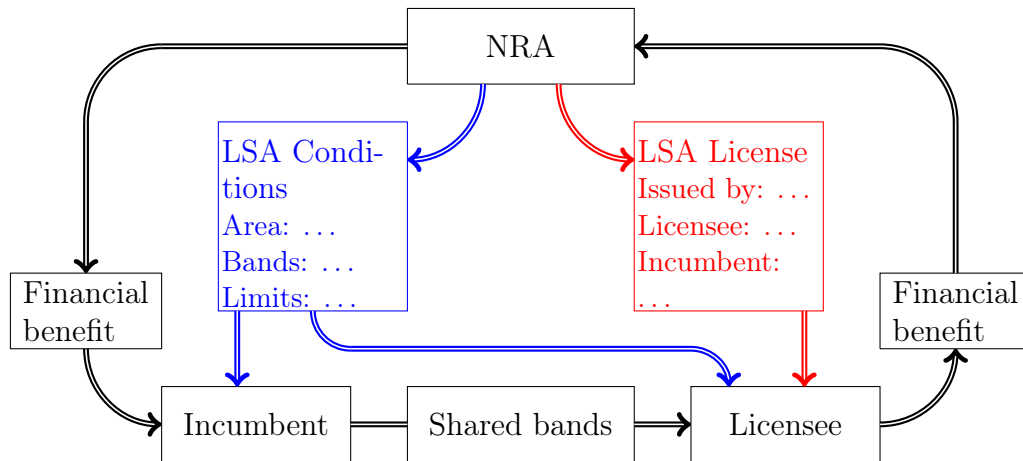


Figure 2.2 Administrative structure of LSA System

ceive sharing rules for specific bands after the sharing agreement is made. It is important to note, that theoretically it is possible for licensee to set limits for band unavailability rate. Therefore, incumbent should not be able to receive monetary gain from radio resources that are unavailable most of the time. However, as it can be seen, most of the interfaces do not assume rapid change of the system parameters. Studies of incentives in LSA-enabled ecosystem were also defined by European Commission Radio Spectrum Policy Group (RSPG) and Nokia in [35, 36].

3. SYSTEM LEVEL SIMULATIONS OF LSA-ENABLED CELLULAR NETWORKS

In this section, brief description of evaluated scenario and will be given, as well as high-level breakdown of the utilized SLS tool. In the end of the section analytical models of single LSA-enabled cell are provided, along with the multi-cell model used for verification of produced results.

3.1 Evaluated scenario

In order to develop and simulate power control methods, a number of modifications to the conventional LSA system architecture were proposed. Introduction of dynamic link between the incumbent (airport), LR and LC will allow incumbent to rapidly update the information in the repository. Thus, when new data is available to the LR, it will notify LC of the changes and the latter will map the updates to the MFCN. It is important to remind, this modification does not contradict the standards defined by ETSI in [33]. As a result, we assume that it is viable to evaluate performance of such system by simulating a dynamic scenario and performing a live trial. Proposed simulation scenario assumes dynamic operation of the system due to the presence of high velocity objects owned by incumbent. Scenario uses Cartesian coordinate system to define locations of the entities. Scenario also assumes that licensee is an operator, that owns LTE MFCN with LSA capability. We assume that licensee already registered LC with LR and successfully obtained LSA License from NRA. MFCN of the licensee is comprised of 25 hexagonal cells that are located in a 5 by 5 cell square. Each cell contains four static UE devices operating on shared bands. For sake of keeping the simulation complexity within reasonable bounds, we do not consider the bands that are owned by licensee. This means, that if the shared bands are unavailable, simulated network will not be able to deliver packets. Apart from the licensee, incumbent is present, his presence is denoted by an airplane departing from the airport near the MFCN.

We assume that airport is located within protection area, meaning that no harmful interference can occur on the receiver of the airport ATC. However, plane travels over MFCN and receiver of the airplane may be affected by the transmissions from

UE equipment. As the plane gains altitude, interference decreases. After plane gained altitude of 2 kilometers, we assume that MFCN users are no longer interfering with the airplane.

In order to define the scenario in more detail, relations and other entities must be defined. Incumbent (ATC) has access rights to update protection information in the LR. This assumption is made since ATC tracks all flights that are destined to the airport and are in proximity. This makes ATC a perfect candidate for rapidly updating radio resource availability information according to the location of the departing airplane. LR and LC are present in the scenario in a form of a single entity, this entity is responsible for controlling UL TX power limits and is linked to the MFCN. This means that the interface between them is omitted and assumed to have insignificant delays and sufficient capacity for rapid updates. LR is supplemented with interference estimator, which is aware of airplane location and calculates the TX power limits for UL channel. In real life this estimator can be implemented as software running on a server within the LR. In terms of parameters, we assume that

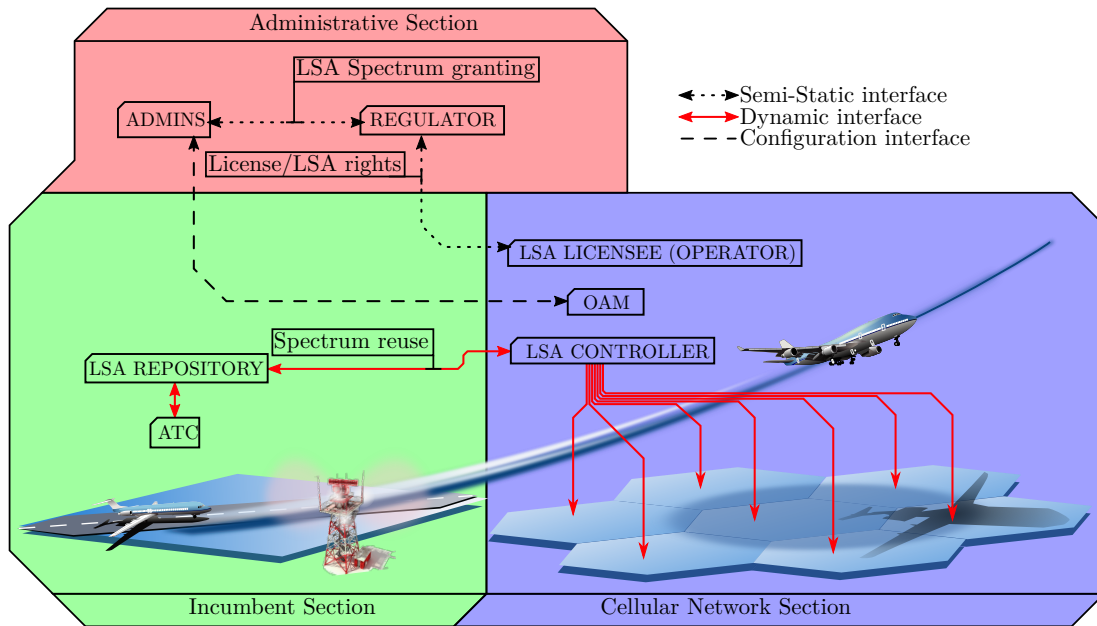


Figure 3.1 Administrative composition of the scenario

MFCN operator uses 5 MHz of shared spectrum for serving the UEs. Coordinates of the devices are uniformly distributed on X and Y axes, while height is fixed to 1.6 meters. BS towers are located in the geometrical centers of the cells and are 15 meters high. Down-tilt angle for the emitters is 15 degrees, while the ISD is 500 meters. As a result, the cells have a radius of 288 meters. At the beginning of the simulation, the airplane has an initial velocity of 230 km/h. It is assumed that airplane just lifted off and starts to gain altitude. Airplane accelerates after takeoff

to reach cruise speed, the takeoff slope is constant and equal to 7 degrees. Velocity of the airplane is updated using equation 3.1.

$$V_{pl}(t) = V_{pl}(t-1) \cdot (1 + 5/V_{pl}(t-1)), \quad (3.1)$$

where $V_{pl}(t)$ is velocity vector of the airplane at current time instance.

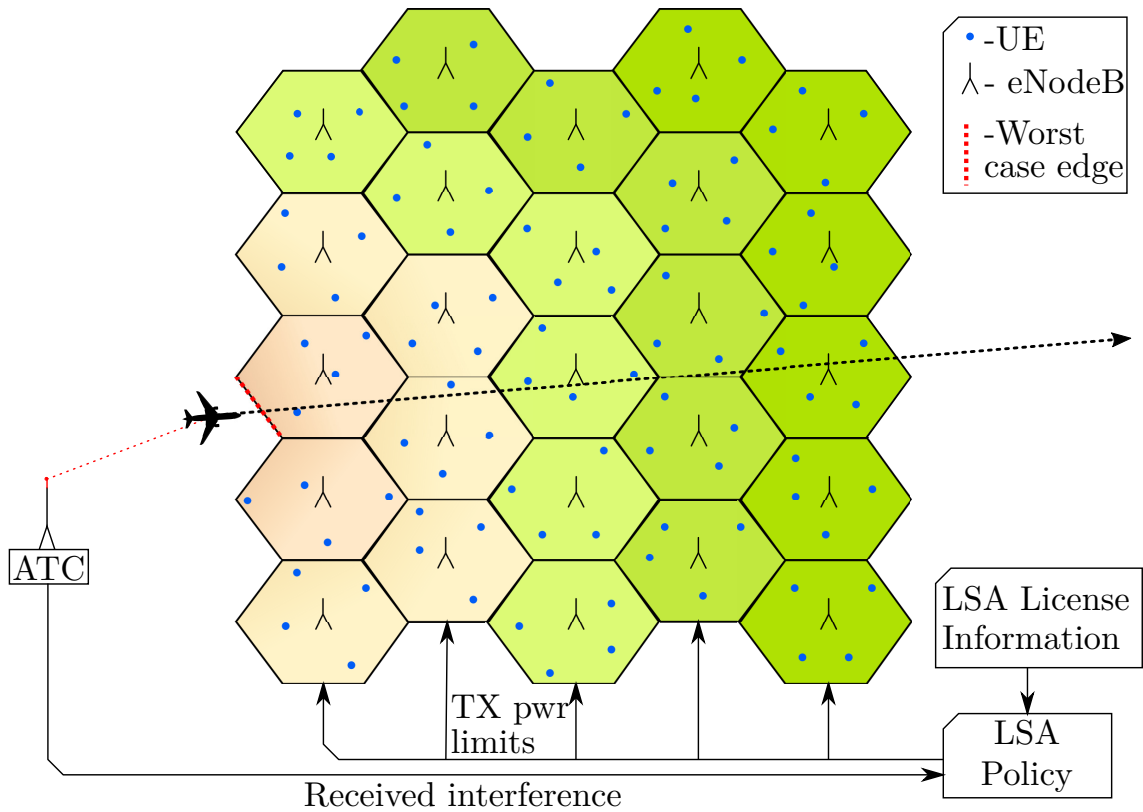


Figure 3.2 Proposed simulation scenario

Interference from each cell is evaluated using equation 3.2. For every cell, we first need to determine whether airplane is above the specific cell. If it is, we calculate the free-space path-loss from ground to plane by substituting airplane altitude instead of distance. This approach assumes that the UE device is always under the airplane and our system considers the worst case in terms of UE location (minimal distance to airplane). However, if the cell in question is not located under the airplane, we must locate the nearest edge of the cell. In Figure 3.1, such edge is marked with red dashed line. After such edge is found, we assume that UE device is located on this edge of the cell in such way, that distance to the airplane is minimal. Once again, this approach allows us to estimate worst case scenario and prevent underestimation of the interference. Free space loss is used for estimation of the interference between

MFCN and airplane since it is assumed that there are no obstacles between airplane and each UE.

$$I_{est} = \begin{cases} P_{TX} - (20\log_{10}(d_{CE}) + 20\log_{10}(f_c) - 147.55), & \text{airplane is not above the cell} \\ P_{TX} - (20\log_{10}(h_{air}) + 20\log_{10}(f_c) - 147.55), & \text{airplane is above the cell} \end{cases} \quad (3.2)$$

where I_{est} is estimated interference at the airplane receiver, P_{TX} is current UL TX power limit at cell of interest, d_{CE} is distance from nearest edge of the cell, h_{air} is current altitude of the airplane and f_c is carrier frequency, on which is used by licensee under LSA license. After the modified LR recalculated the interference estimate, UL TX control method can be applied by the LC. For starters, we will see how simple SHUTDOWN method works. This method can be applied at any instance when estimation is updated. This means, that application of the method and update of TX power limits occur at certain time instances. That explains the use of discrete time in the equation 3.3. SHUTDOWN method verifies if current TX power level in certain cell could cause harmful interference with the incumbent. If calculation results indicate a chance of harmful interference from certain cell, shared bands are getting disabled in that cell. This means that all devices that operate on shared bands will experience connectivity loss.

$$P_{TX}[n] = \begin{cases} -80dBm, & I_{est} \geq I_{thr} \\ P_{TX}[n-1], & I_{est} < I_{thr} \end{cases} \quad (3.3)$$

where $P_{TX}[n]$ is UL TX power limit calculated at time instant n , I_{est} is estimated interference at the airplane and I_{thr} is interference threshold defined by LSA license agreement. Another viable option is limiting TX power instead of completely disabling the cell completely. This method is called LIMIT POWER. It calculates how much interference is caused by each cell and decreases UL TX power limits in each cell. Reduction of TX power is made in one single step by subtracting difference between I_{est} and I_{thr} from $P_{TX}[n-1]$. This method provides the benefit of keeping the network operational while adhering to the license requirements. However, a different approach can be taken. In LIMIT POWER, the interference is calculated for one individual cell. Therefore, method was focused on limiting the interference from individual cells, rather than from networks. SMART LIMIT method was developed from LIMIT POWER, in which interference from whole network is used as key criteria. This is beneficial in a way that it is more closely related to the goal that was

set for all of the methods. SMART LIMIT attempts to decrease interference from the whole network, rather than from individual cell. However, this method does not complete the configuration of the network as fast as previous ones. SMART LIMIT reduces UL TX limit for most harmful cell on each iteration until the total interference is below configured threshold. It is shown later in the thesis, that introduction of dynamic stepping decreases number of loops the system must complete in order to reach satisfactory conditions. Pseudo-code representation of the algorithm without checks for invalid input is given below.

3.2 Simulation toolkit description

A custom-made system level simulator (SLS) called WinterSIM was used to simulate the aforementioned scenario [37]. The simulator was developed with WINTER group members and passed verification with 3GPP LTE calibration data. SLS tool has modular structure in order to ease the development and prototyping of novel solutions. Most of the code is written in Python 3.4-3.6, physical model of the channel is written in C++ and supplementary scripts, such as slow fading generator, are written in Octave script. Simulation software supports creation of custom traffic generators, such as CBR, saturating and Poisson session generators. Interfaces and can also be extended to simulate custom medium access control (MAC) protocols. Moreover, the simulator is capable of detecting and estimating interference between two UE terminals in radio networks. Furthermore, LTE power control mechanisms that depends on current network status are also implemented in the simulator (SINR target policy, for example). As of now, the development of the simulator continues towards supplementing mmWave communications module with fully functional MAC layer and proper channel models for scenarios varying from on-body links between wearable devices to massive deployments with multiple UEs and access points (APs). Apart from that, simulator is also capable of taking into account mobility of the nodes. Multiple mobility models are implemented in the simulator, such as random walk, random way-point and random direction. General structure of the simulator can be seen in Figure 3.3. SLS supports saving the results to both Matlab files and NoSQL database (such as MongoDB) for post-processing. In this particular study, MongoDB was used, since parsing and processing of data was easier to implement in Python. This is so, since numerous scientific libraries are available for Python (NumPy, Matplotlib and SciPy) [38] and plot styles can be adjusted to have a seamless appearance in the thesis. As for the input data, the SLS is able to load 2D directivity patterns of antennas from image files, in order to reduce simulation time of the scenario. SLS can also improve the accuracy of the results by performing multiple MC trials. During each trial replications are performed

in order to decrease variance of the resulting statistical data.

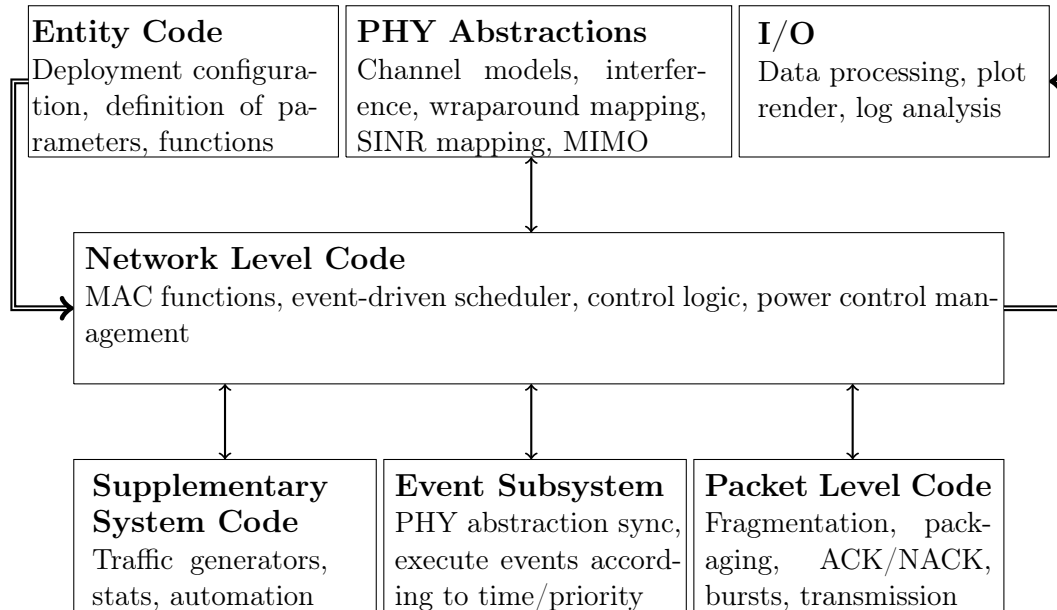


Figure 3.3 General structure of the simulator

For this study, most of the modifications were introduced at Entity Level Code, Event Subsystem, Network Level and in the main loop of the SLS. Custom scenario with 25 cells and a highly mobile airplane entity were implemented on the Entity level. This was done in such way, since simulator assumes that each scenario must be defined in single file, which specifies which modules and parameters must be used. LSA entities were also implemented on entity level and were not deeply integrated into the SLS, in order to prevent bloating of the software. A new “dummy” interface was created on Entity Level in order to measure received interference at the airplane. This interface logged all received data packets from MFCN and calculated received power over 1 second. It is important to note, that the interface measured received energy based on the duration of the received message. In other words, the interface estimated the duration of the message and based on that estimated amount of energy it delivered. When the simulator had to store the interference information, it was estimated, how much energy arrived during one second in total, and from that the interference power was calculated. This data was then saved and used to verify the correct operation of the UL TX power control. It is important to note, that all data packets that were detected on shared bands are assumed to cause harmful interference to the airplane. Furthermore, in order to decrease simulation times, computing cluster support was added to the software. Slurm cluster management system [39] was used as a backbone, since the documentation for it was well-written and it provided required functionality (task tracking, load distribution). A cluster

computing environment was also configured to perform the simulations. Computing environment was comprised of heterogeneous machines placed in Tampere and St. Petersburg. Two sites were connected via OpenVPN tunnel with open shortest path first (OSPF) routing protocol enabled. GlusterFS 3.8.6 [40] in redundant array of independent disks (RAID) of level 5 was picked as a storage for home directories where SLS code was located. It was selected because of configuration flexibility, good scalability and ease of configuration.

3.3 Verification and analytical results

In order to verify results and study long term performance of the system, multiple analytical models were developed. They will be briefly demonstrated in this section of the thesis. First model was built from basic queuing theory entities and analyzed with Markov chains [41]. Representation in terms of queuing theory can be seen in Figure 3.4. It was aimed at estimating performance and blocking probability of one cell over a long period of time at various shared band failure/recovery rates. System was analyzed in terms of average number of users and probability of user arriving while shared bands are unavailable. In order to take into account multi-user capability, model employs a server pool with capacity C , which can be seen in dashed rectangle in Figure 3.4. Apart from that, a finite queue with capacity r is present to store user requests. It is important to note before continuing that $r > C$. If request arrives into the system when all of the servers are occupied and queue is also full, it is considered to be lost. When shared band is revoked from the cell (failed), all requests in the server pool are paused and stored in the queue. After shared bands recover and return back in service, paused tasks gain elevated priority over other.

From the results of the simulation it was determined that arrival rate of the users does not affect the performance of the system as much as the failure/recovery rates α and β . This actually explains why deployment of LSA-enabled systems might not be feasible near highly congested airports, in case telemetry bands are reused.

Second model of single-cell LSA deployment was based on assumption that apart from shared band, MNO has access to his own licensed band [42]. This meant that the system should be less sensitive towards shared band outage. System was represented with two server pools:

- Reliable server pool – used to simulate reliable bands of the MNO. Pool has

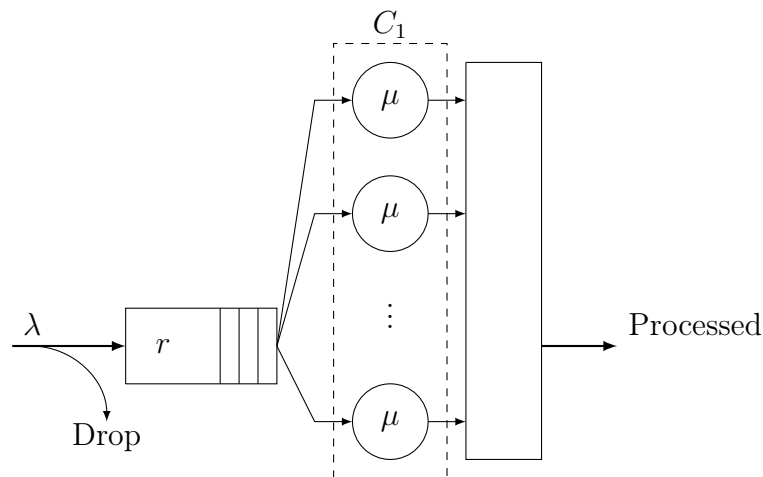


Figure 3.4 Single-cell, single-band LSA model

capacity C_1 in order to simulate limited amount of resources available to users with fixed demand.

- Unreliable server pool – used to simulate shared bands available to the MNO under LSA license. It is important to note that capacity C_2 of this pool was lower than capacity of the reliable pool. This was so, since usually shared bands are smaller than the bands that are licensed to the MNO.

Both pools share single queue of capacity r and have similar processing rates. However, priority of the reliable pool is higher, meaning that user requests are first forwarded to it. After reliable pool is occupied, requests are forwarded to unreliable pool, if this pool is also full, requests are dropped. If unreliable pool shuts down, all requests that are currently served by it are relocated to reliable pool. If some of the requests do not fit into the pool, they are moved to the queue. If the queue is also full, these requests are considered to be lost.

Metrics such as mean number of requests in the queue, non-interrupting and blocking probabilities were studied in the work. Non-blocking probabilities were studied from two viewpoints:

- Probability P_1 that there is at least one user served on shared bands, and their service will not be interrupted during evacuation to licensed bands (reliable pool). This corresponds to cases when MNO does not need to interrupt service of any users, since none of them are served on shared bands or there are slots available for evacuation in the reliable pool.
- Probability P_2 that service of certain user will not be interrupted. In contrast to P_1 , this probability demonstrates how QoS of single user is affected by LSA.

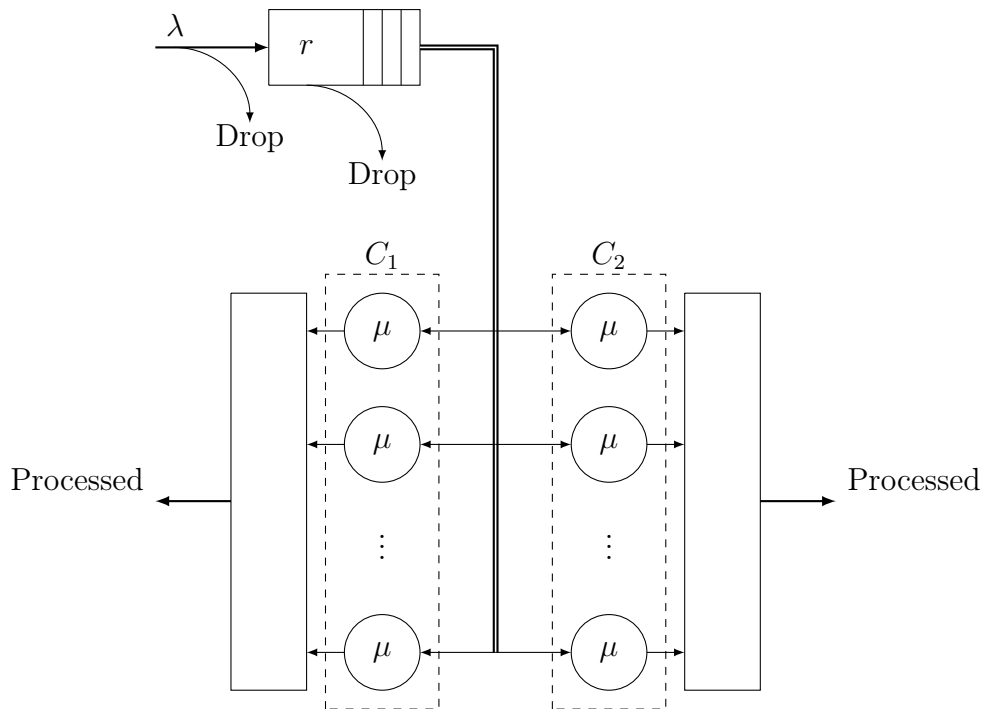


Figure 3.5 Single-cell, two-band LSA model

- Probability F of second pool being unavailable.
- Probability B that service was denied and user request was dropped.
- Average number of requests in the queue Q .

It was determined that such system has a set of optimal parameters, such that P_1 and P_2 are maximized. Generally, it was deduced that we can split parameter set into three subgroups:

- Optimal performance set which corresponds to a balance between loading all of the shared bands and being able to evacuate them to the licensed bands if need arises. Cell is loaded enough to occupy shared bands, but licensed bands and queue may also provide slots for evacuated requests.
- Underloaded state, when all of the requests are served, but shared bands are not utilized at all. This case is suboptimal, since if shared bands are not used, they are not strictly required in the system. This might be considered as an exception, but MNO should study the parameters of its network prior to enabling LSA. Otherwise, apart from wasting bands operator will also waste financial resources, since no users are served on these bands.

- Overloaded state, when both shared bands and licensed bands are loaded and no vacant slots are available in the queue. This situation is also suboptimal, since in this case users are unable to evacuate when shared bands fail. Therefore it is detrimental for QoS of the system.

Apart from two models mentioned above, another model was created to evaluate performance of specific policy in case of multiple cells. It is important to note, that this model does not evaluate the performance of the system from UE perspective. This is so, since we assumed that distance from UE in the cell and the plane is minimal. This leads us to two possible scenarios:

- UE is on the edge of the cell, which is closest one to the airplane. This situation is assumed to occur when airplane is not above the cell, but is passing near it.
- UE is below the airplane. This scenario can only occur when airplane is above the cell of the UE.

In order to verify correctness of the model, we performed simulation of the scenario seen of Figure 3.2. As a result, we obtained a curve which corresponds to the minimum UL TX limit set in the network. Aforementioned plot can be seen in Figure 3.6, on it minimum UL TX limit in cells, that airplane flew over, is given individually, as well as minimum of values produced by the analytic simulation in each cell.

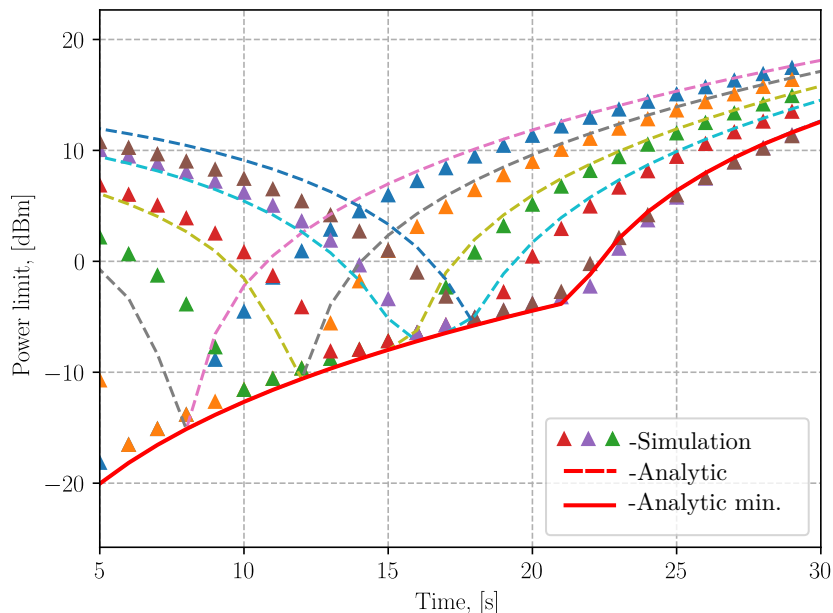


Figure 3.6 UL TX power minimum in simulation and analytic model

4. UPLINK TRANSMISSION CONTROL METHODS

In this section, proposed control methods for uplink channel will be described. Their impact on network performance and performance metrics will also be studied and discussed. In the end of this section a small optimization is introduced in one of the algorithms to reduce number of steps, required to reach satisfactory state.

4.1 Implemented control methods

During the studies multiple control methods were considered and evaluated. In total, four methods were created:

- **IGNORE** - method that was used to prove the necessity of control. No action is taken by the LC when this method is active. It does not affect the network operation at all and demonstrates that harmful interference will be experienced by the incumbent.
- **SHUTDOWN** - simplistic method that guarantees satisfaction of license conditions. In this method, LC estimates interference received by incumbent from one cell, if it exceeds threshold, aforementioned cell is deprived of shared bands. In reality this will most probably mean that LC will interrupt service on shared bands by roaming all UEs to licensed bands and disabling service on shared bands. Roaming step may be necessary, since this may make the transition less abrupt for UE. Service on shared bands is restored when estimated interference is below the threshold. While this method prevents harmful interference to the incumbent, it also cripples LSA operation in interfering cell. Roaming will only be possible if licensed bands are not overloaded. If this does not hold, this method leads to poor QoS and QoE and thus, is not particularly suitable for sensitive applications.
- **LIMIT POWER** - transmission control method that aims at improving QoS and quality of experience (QoE), compared to SHUTDOWN method. System

estimates total interference from specific cell and applies a certain penalty to the UL TX power limit. Penalty P_{pen} is calculated as follows:

$$P_{pen} = \begin{cases} 0, & I_{est} < I_{thr} \\ I_{est} - I_{thr}, & I_{est} > I_{thr} \end{cases} \quad (4.1)$$

where I_{est} is estimated interference and I_{thr} is interference threshold configured according to the LSA license.

- SMART LIMIT - method that is aimed to reduce interference towards incumbent services by solving a global optimization task. Contrary to LIMIT POWER, in this method network is considered as a whole and cells that cause most of the interference are penalized in terms of UL TX power limit. Algorithm behind this method runs a number of iterations before applying final penalties to the network. Python code of the core function of the method can be seen in the listing below.

Program 4.1 LIMIT_POWER algorithm

```

1 # Calculate new TX power limits
2 # cells - list of cell objects, stores coordinates,
3 # current TX power limits for UL, number of UE devices
4 # airplane - airplane object, stores coordinates of the plane
5 # thresh - current interference threshold, if it is breached,
6 # policy has failed
7 # to satisfy LSA license conditions
8 def dyn_update(cells, airplane, thresh):
9     interfs = list()
10    while(True):
11        for i in cells:
12            # iface of each cell is the radio interface serving
13            # shared band pos is a physical position of the node
14            interfs.append((i.iface, MAX_TX_PWR, \
15                FSPL(i.pos, airplane.pos)))
16            if thresh > assert_interf(cells, airplane):
17                break
18            # We sort the interference tuples, so that most harmful
19            # cell is first in the list
20            interfs = interfs.sort(key=lambda t: 10.0**((t[1] - \
21                t[2])/10.0), reverse=True)
22            interfs[0] = (interfs[0][0], interfs[0][1] - step, \
23                interfs[0][2])

```

- SHANNON - method that is aimed at maintaining best possible performance of the network while keeping the interference below threshold. Previous meth-

ods were inconsiderate towards UE operation and outage. Previous methods did not estimate the consequences of penalty application and whether we can avoid outage by penalizing another cell. SHANNON method uses Shannon-Hartley equation to estimate maximum transmission rate of the channel after reconfiguration in order to prevent outage of the UEs that experience worst channel conditions (“worst” UEs). It must be configured with both interference threshold and rate threshold. During operation, if interference threshold is breached by certain cell, we calculate if reducing UL TX power will reduce maximum transmit rate of “worst” UE drop below threshold. If it does, we attempt to decrease interference by applying this method to neighboring cell. After these steps are performed, we estimate whether application of the method dropped interference value below threshold. If it did not, and maximum transmit rate of the “worst” UE dropped to the threshold, we disconnect the “worst” UE, reduce power limit and select a new “worst” UE. This approach was only tested during the LSA trial in BUT. Code listing for it can be found below, code was taken from the BUT oracle script.

Program 4.2 SHANNON algorithm

```

1 def run_throughput_iteration(self):
2     self.bs_powers = self.bs_powers_init.copy()
3     nn = len(CELL_COORDS)
4     nearest_ue_pl = np.full(nn, np.inf)
5     ue_bs_pl = np.full(UE_LOC_BS.shape[0:2], np.inf)
6     ue_bs_pl = ma.array(ue_bs_pl, mask = UE_LOC_BS.mask[:, :, 0])
7
8     for c in range(nn):
9         for i, ue in enumerate(UE_LOC_BS[c]):
10            if ue_bs_pl.mask[c, i]:
11                continue
12            pathloss = get_pathloss(self.airplane_coords[0:2], ue)
13            nearest_ue_pl[c] = min(nearest_ue_pl[c], pathloss)
14            ue_bs_pl[c, i] = get_pathloss(CELL_COORDS[c, 0:2], ue)
15
16     ue_throughput = ma.array(np.zeros(ue_bs_pl.shape), \
17     mask=ue_bs_pl.mask)
18
19     for c in range(nn):
20         for i, ue in enumerate(UE_LOC_BS[c]):
21            if ue_throughput.mask[c, i]:
22                continue
23            ue_throughput[c, i] = Shannon_estimate(W / len(UE_LOC_BS[c]),
24            self.bs_powers[c] - ue_bs_pl[c, i]) / 1e6
25

```

```

26  step = 0
27  total_interf = RATIO2DB(DB2RATIO(self.bs_powers -\
28  nearest_ue_pl).sum())
29
30  while total_interf > INTERF_MAX and step < self.max_steps_fwd:
31  ue_throughput_diff = -ue_throughput
32  for c in range(nn):
33  p = self.bs_powers[c] - self.power_step
34  for i, ue in enumerate(UE_LOC_BS[c]):
35  if ue_throughput.mask[c, i]:
36  continue
37  if p >= -30:
38  ue_throughput_diff[c, i] += Shannon_estimate(W /
39  len(UE_LOC_BS[c]), p - ue_bs_pl[c, i]) / 1e6
40  else:
41  ue_throughput_diff[c, i] = 0
42
43  thr_deriv_metric = ue_throughput_diff.sum(axis=1)
44
45  assert (thr_deriv_metric <= 0.0000000001).all(),\
46  "Power derivative must be non-positive!!!"
47
48  metric = nearest_ue_pl * ((1 - thr_deriv_metric) ** ALPHA)
49
50  # m0 = thr_deriv_metric.argmax()
51  m1 = metric.argmin()
52  print("metrics: {}, {}, {}, reducing power on {}".format(
53  nearest_ue_pl, thr_deriv_metric,
54  metric, m1))
54  self.bs_powers[m1] -= self.power_step
55
56  total_interf = RATIO2DB(DB2RATIO(self.bs_powers - nearest_ue_pl
57  ).sum())
57  step += 1
58  print("Found configuration {} in {} steps".format(self.bs_powers
59  , step))

```

After the simulation, plots of various performance metrics were made, most informative are the heat-maps for UL TX power for various control methods. They help us understand how the situation in the scenario progressed as the incumbent-owned object traveled away from the deployment. Apart from heat-maps, interference plots will be given to compare different policies for power control. Heat-maps below correspond to SMART LIMIT method, since it is more complex than IGNORE and SHUTDOWN.

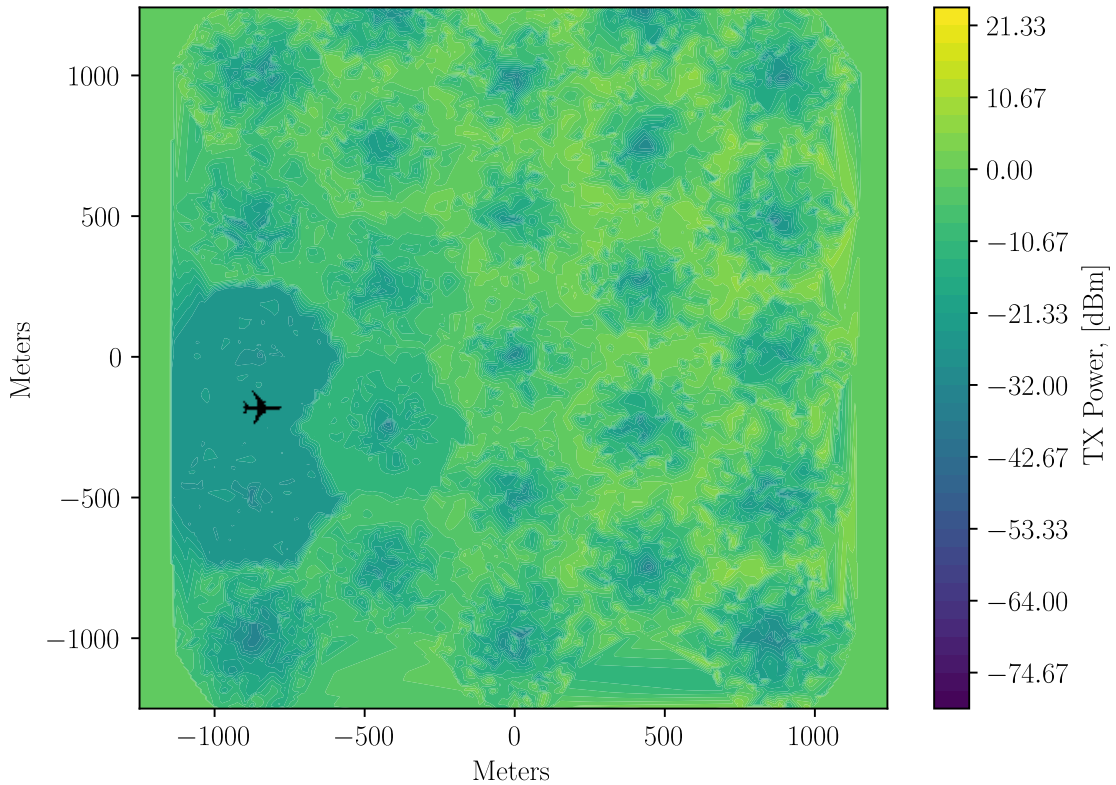


Figure 4.1 UL TX power at 5 seconds

Figure 4.1 shows TX power values at five seconds after plane takeoff. Evidently, the altitude of the airplane is low and severe power limits are applied to the border cells of MFCN.

Figure 4.2 is dedicated to time instance when airplane is above the geometrical center of the MFCN, it can be seen that the impact of the power control method decreased. This is because the airplane gained altitude and minimal distance to the closest UE has increased.

One could assume, that the UL TX power limit mask, that is applied to the cell is not symmetrical. However, it is not so, the slight trace, that is left after the plane moved away from interfering cell, appears due to the transient in the cells. This

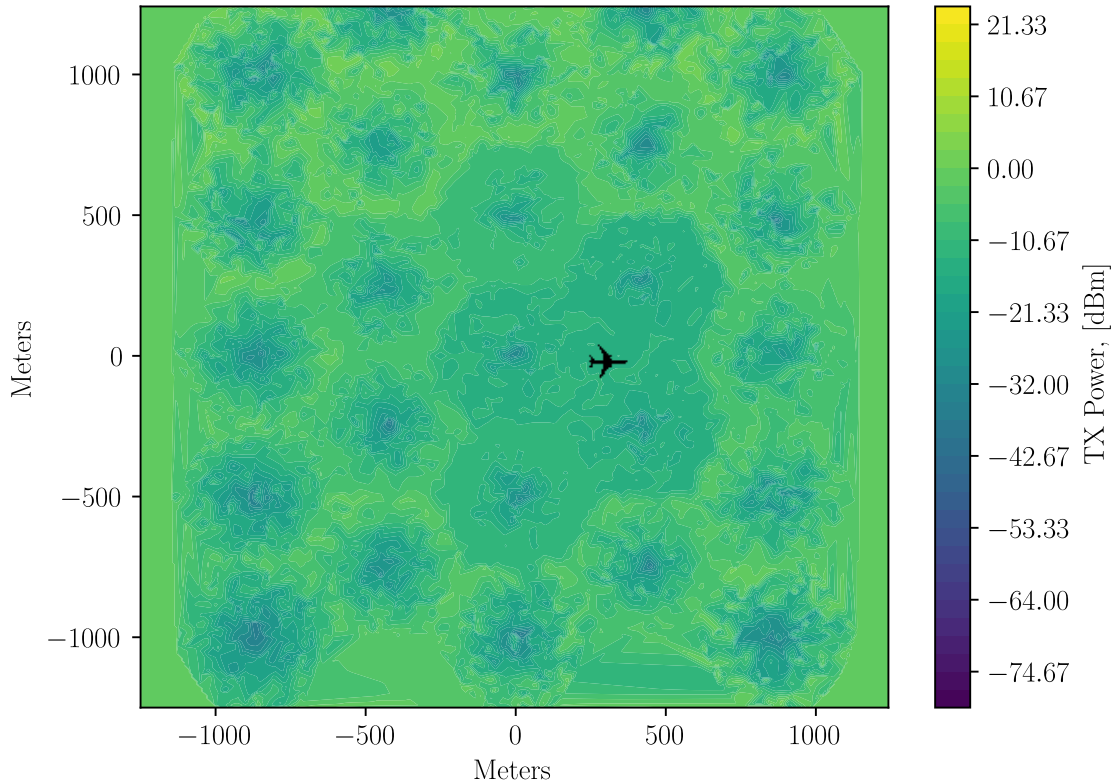


Figure 4.2 UL TX power at 15 seconds

transient is caused by the fact that power control algorithm of the MFCN is focused on reaching specific SINR. When airplane is in the vicinity, power control algorithm is limited by the UL TX power limit imposed by LSA. After the limit is raised, power control starts gradually raising power. Moreover, since the SINR depends on interference from neighboring cells, transmit power in cell will increase when its neighbors are no longer limited by LSA incumbent. Because of these two factors, actual UL TX power is increased gradually until the SINR conditions are satisfied in all of the cells. Increase occurs gradually also because LSA-related power control does not enforce update of the actual UL TX power, and rather sets the upper limit for MFCN power control. Therefore, transmission rates in the network may also update slower than actual UL TX limits, since UE will not be able to use certain MCS before reaching acceptable SINR value.

On this page, UL TX power heat-map is given for time instance, when airplane is over the right edge of the deployment. It can be seen, that the limit applied to the cells below the airplane are higher than at the beginning of simulation. This, once

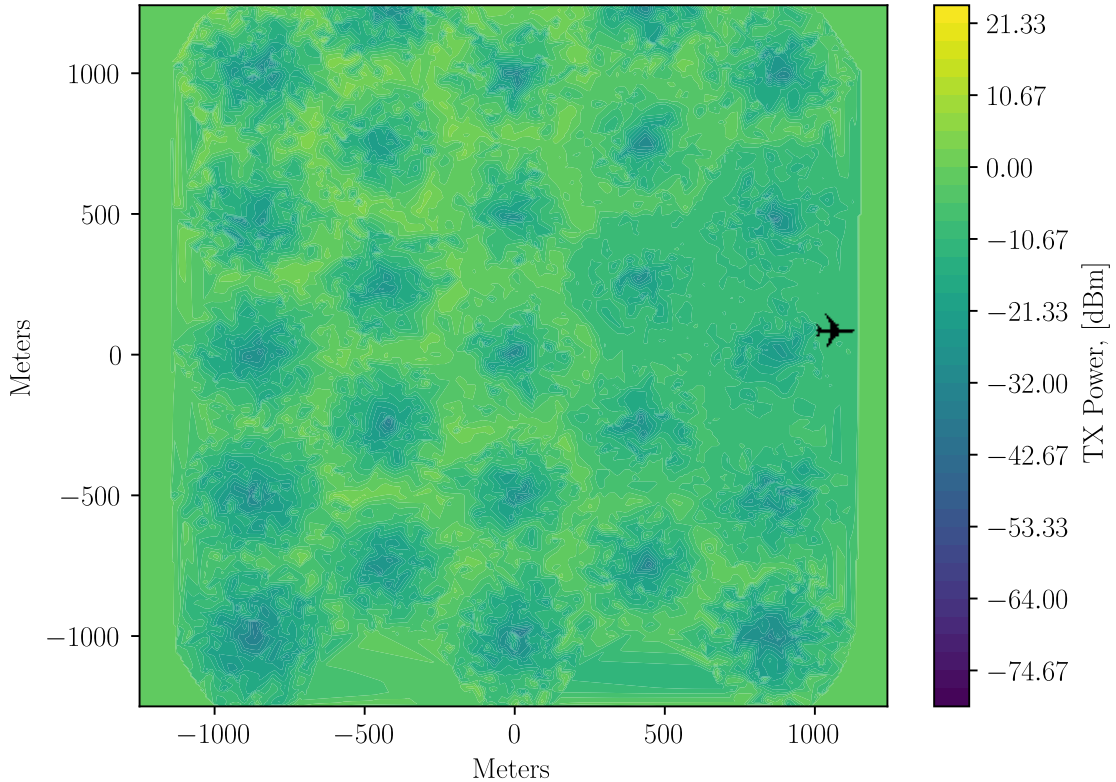


Figure 4.3 UL TX power at 20 seconds

again, is due to the increase of shortest distance from airplane to nearest UE. Apart from the increase of UL TX power limit, we can observe that number of affected cells also decreased.

4.2 Power control evaluation

In order to be more specific regarding the performance of the methods, let us study plots of interference and UL TX power limits. These plots help us understand whether certain method failed to comply with the requirements we set in the scenario. Also, they will help us see how did UL TX power limit change during the simulations. In total, this information will let us analyze the performance of the methods from position of both operator and incumbent

First, we will examine mean UL TX power for all four methods. As it is seen on the plot, IGNORE method does not decrease the power limit. In fact, the UL TX

power increases over time due to the fact that internal power control of the network is configured to maintain certain SINR. After simulation started, power control mechanisms attempt to reach SINR by increasing TX power. Other methods decrease power limit in the network to prevent violation of LSA license conditions. SHUTDOWN method terminates service in cells as the plane travels over the deployment. After plane leaves the area, service is resumed in cells, that are no longer interfering with incumbent. Both LIMIT POWER and SMART LIMIT show similar behavior, they gradually decrease UL TX power limit until interference is estimated to be within acceptable range.

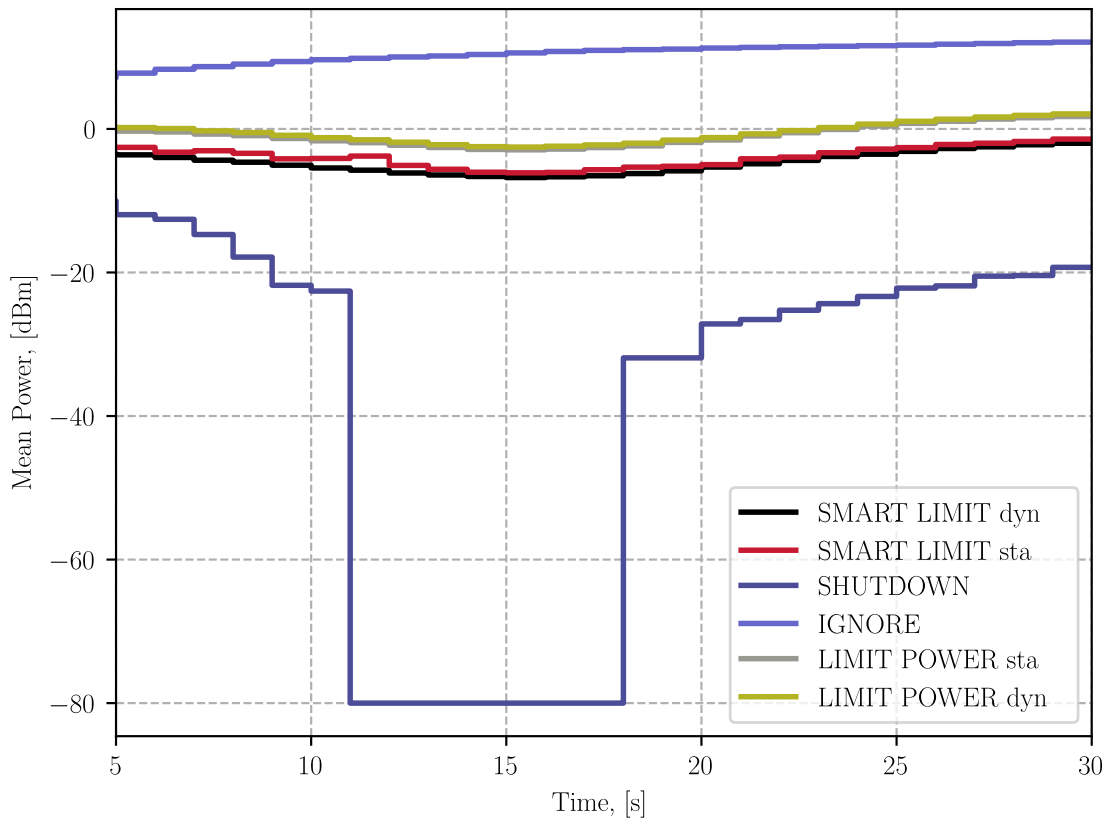


Figure 4.4 Average UL TX power limit

Figure 4.5 shows how interference received by the airplane changed during the simulation. As it can be seen, IGNORE method failed to satisfy LSA license requirements. From this, we can deduce that power control is indeed required in order to prevent service degrading on incumbents side. We can also see that all other policies manage to keep the interference below threshold. However, SHUTDOWN can be considered overprotective, since it terminates service even if interference exceeds limit by a small amount. LIMIT POWER and SMART LIMIT are more adequate

in this regards, since they estimate adjustments needed for reaching satisfactory conditions.

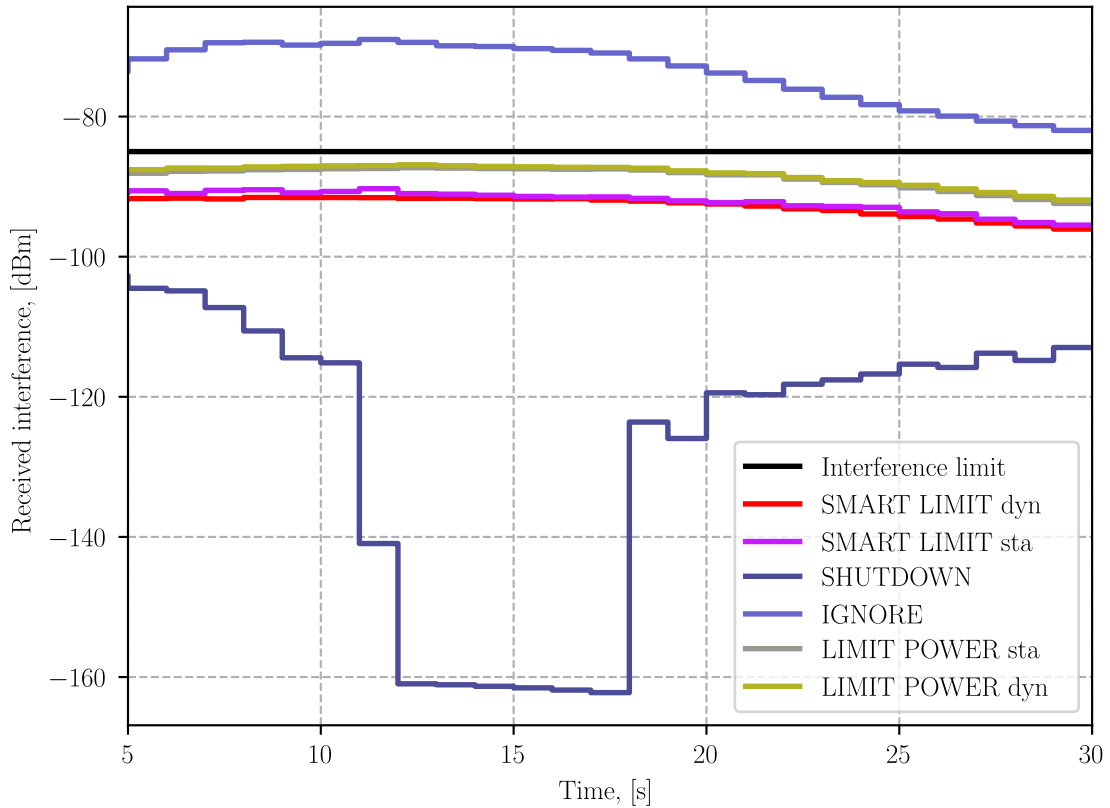


Figure 4.5 Interference received by an airplane

It may seem odd that at the end of simulation UL TX power increases, while interference decreases. However, it is explained by the fact that distance between airplane and nearest cell increases. This means that after airplane left airspace over deployment, power limit is increased, but internal power control mechanism did not yet increase UL TX power.

4.3 Algorithm performance evaluation

As it was mentioned before, SMART LIMIT control method was optimized to reduce number of steps. Optimization was performed by calculating a power reduction step depending on the margin between interference threshold and currently estimated

interference. Reduction step was defined with equation given below:

$$I_{dyn} = \begin{cases} 2 \cdot \log(I_{est} - I_{lim}) & I_{est} - I_{lim} > 1 \\ I_{est} - I_{lim} & I_{est} - I_{lim} \leq 1, \\ 0 & I_{est} - I_{lim} \leq 0 \end{cases} \quad (4.2)$$

where I_{dyn} is the reduction step that will be applied to the cell, I_{est} is the estimated interference and I_{lim} is the interference threshold. As we can see, when interference excess is higher than 1 dB, step size increases logarithmically. However, if excess is less or equal to 1 dB, we must apply linear function, since previous logarithmic function would return incorrect step size. If no interference excess is present, interference reduction step is zero.

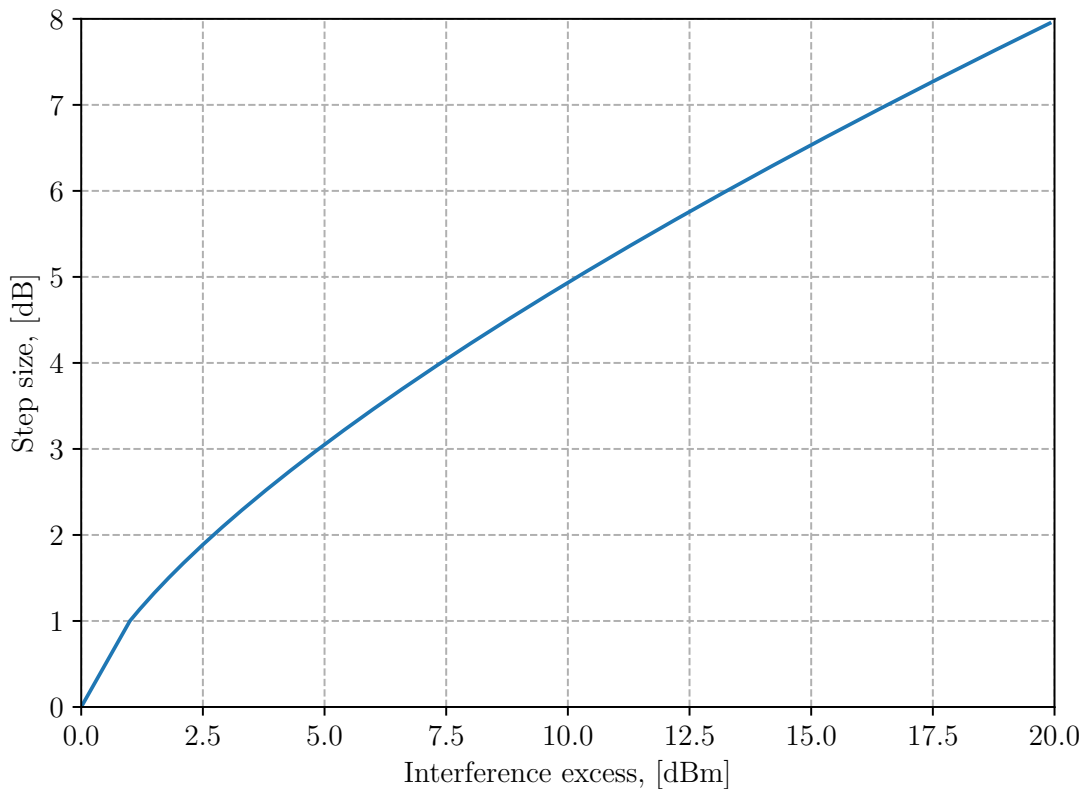


Figure 4.6 Dynamic stepping curve

It may seem that this optimization will result in more overheads, since logarithms, branching and multiplications are used. However, as of now it is possible to use specialized hardware that may reduce effects of these operations on overall perfor-

mance. On the other hand, Figure 4.7 demonstrates, that reduction in number of steps is significant. In worst case, when difference between interference limit and actual interference is small (end of the simulation), dynamic stepping requires approximately 3.5 times less steps than static stepping. Apart from that, we can see that variance also decreases significantly, which in turn means that computation time will be more predictable.

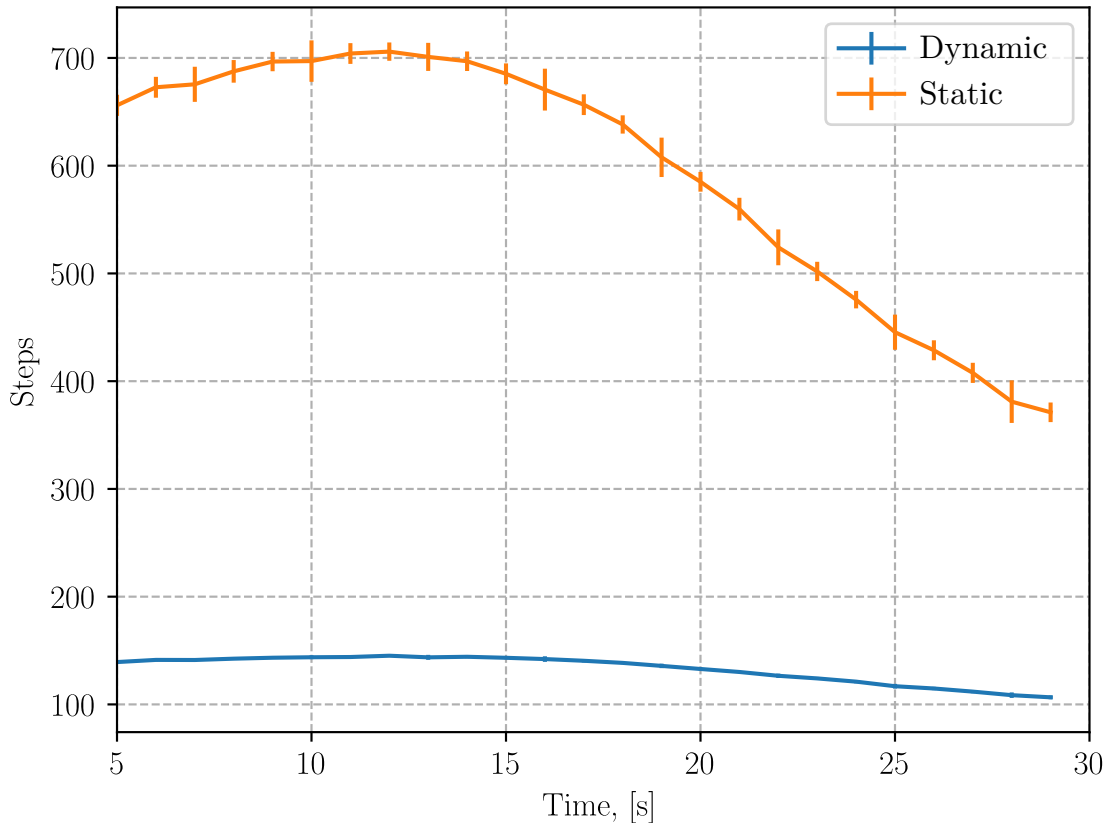


Figure 4.7 Number of steps taken to reach satisfactory conditions

If we look into the problem from another perspective, we will notice that concept such as multi-access edge computing (MEC) is mentioned as one of the possible enhancements in 5th generation networks (5G) [43]. This concept is based around improving computationally expensive services by relocating application hosting hardware to the frontier of the network. This way, MEC strives to deliver lower latency of the applications. Lower latency is explained by the fact that path between application client and server has less hops than without MEC. In spite of this, it is important to note that 5G also assumes that count of always-on users per cell may range from thousands to millions [44]. Therefore, we may need to increase computational power in order to handle multiple update of the power limit for individual cells or users. According to Amdahl's law, we might not be able to reach linear increase

in performance of the system, but we will be able to localize and limit computations to the domain that is currently shared between licensee and incumbent.

5. PRACTICAL OPERATION OF LSA-ENABLED CELLULAR SYSTEMS

In this section, results and specifics of trial in Brno will be given. These will include description of the network, server and client descriptions for traffic generator programs.

5.1 Deployment and equipment

In order to observe how our algorithms perform in the field, we organized a test trial with team from BUT. During the trial we tested two power control methods for LSA-enabled MFCNs, SHANNON and SMART LIMIT. Trial was performed on one of the floors of the BUT, which had a cellular network deployed on it. During the trial, several modifications and additions were made to the LTE network of BUT. As it was stated in the beginning of the thesis, modifications did not conflict with the conventional LSA system structure. To test the algorithms, we focused on testing power control policies in UL channel and evaluated the availability of that channel over the shared bands. In order to be more specific, Table 5.1 of network parameters is given below.

Description	Value
Release Version (3GPP LTE)	Release 10
Multiplexing type	Frequency division duplex (FDD)
Number of cells (eNB)	3
Band (Frequency)	17 (700 MHz)
Bandwidth	5 MHz
eNB TX power range [MIN;MAX]	[0;-30]dBm
Interference threshold	-85 dBm

Table 5.1 Parameters of the BUT LTE network

Despite the fact that original simulation scenario operated at frequency of 2100 MHz, we were limited in terms of band selection. This was because university test network was not the only LTE network, local MFCN of commercial operator was

also active and we had to avoid interference. We also had to consider that setting the maximum TX power for specific cell lower than -30 dBm would effectively disable it. This was a hardware limitation of the network and this limit could not be changed in software.

Every UE ran a special client application that communicated with the server located in TUT. Communication was handled over transmission control protocol (TCP) socket, and was used to send benchmark data to the server (thus, every UE used UL channel of the system). Both UE and server logged the packets and saved the statistics into a file encoded in javascript object notation (JSON). Operational diagram of the client is shown in Figure 5.1. This was done in case either server or UE malfunction occurs and the logs are lost. Or, if there is a need to update UE with another read-only memory (ROM) image for other experiments at BUT. The benchmark data mentioned above is a stream of bytes from random number generator. Stream was configured to have a constant bit-rate (CBR data generator) of 512 kbps. If amount of radio resources was sufficient, UE was able to keep sending the data to the server. If the quality of the link degraded, due to TX power limitations, and throughput of the channel was no longer high enough, UE was forced to terminate connection. This was done in such way, since it was important to evaluate the dynamic operation of the shared band. Initially, client was written in Python language and ran on a set of computers in early testing phase. Later, client was ported by Kryštof Zeman in Brno to Android OS.

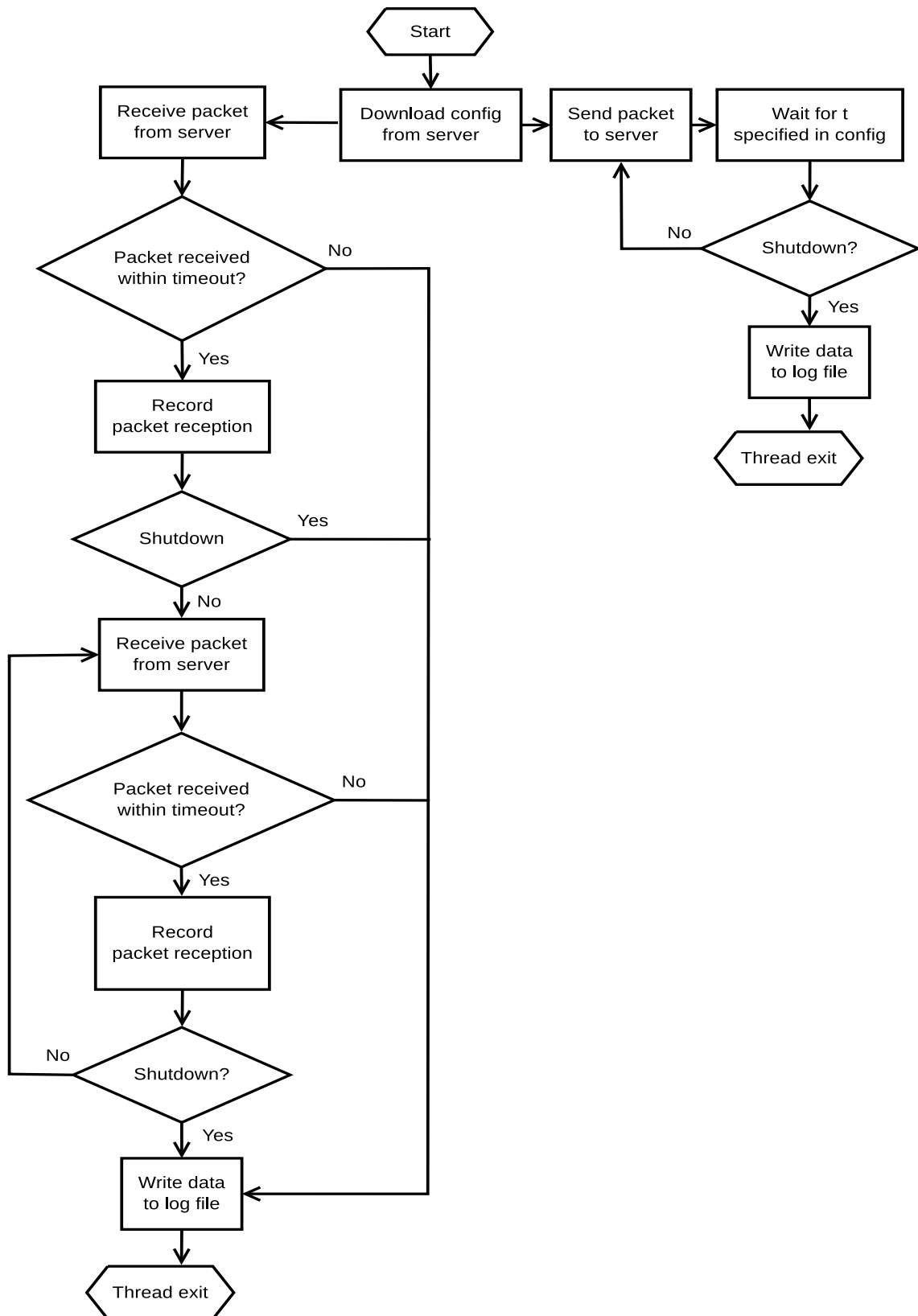


Figure 5.1 Operational diagram of client application

Server in TUT was kept operational for keeping logs of received data packets and configuring newly connected UEs. Connecting UEs must provide their IMSI to the server, so that the latter one can add them to the dictionary of connected users. After that, experiment parameters are sent out as a set of three integers (namely requested rate, number of requests to send and session token). Program was running on *Simhost* server, provided by W.I.N.T.E.R. research group. Server was connected to the Internet via 1 Gbps ethernet link, that guaranteed that measured characteristics will not be affected by performance of the server interface or network. This was further verified by running *iperf* to test throughput of the link. Operational diagram for server can be seen in Figure 5.2. Reference implementation of the server was written in Python and did not utilize any encryption mechanisms, since number of attack vectors and their potential were low.

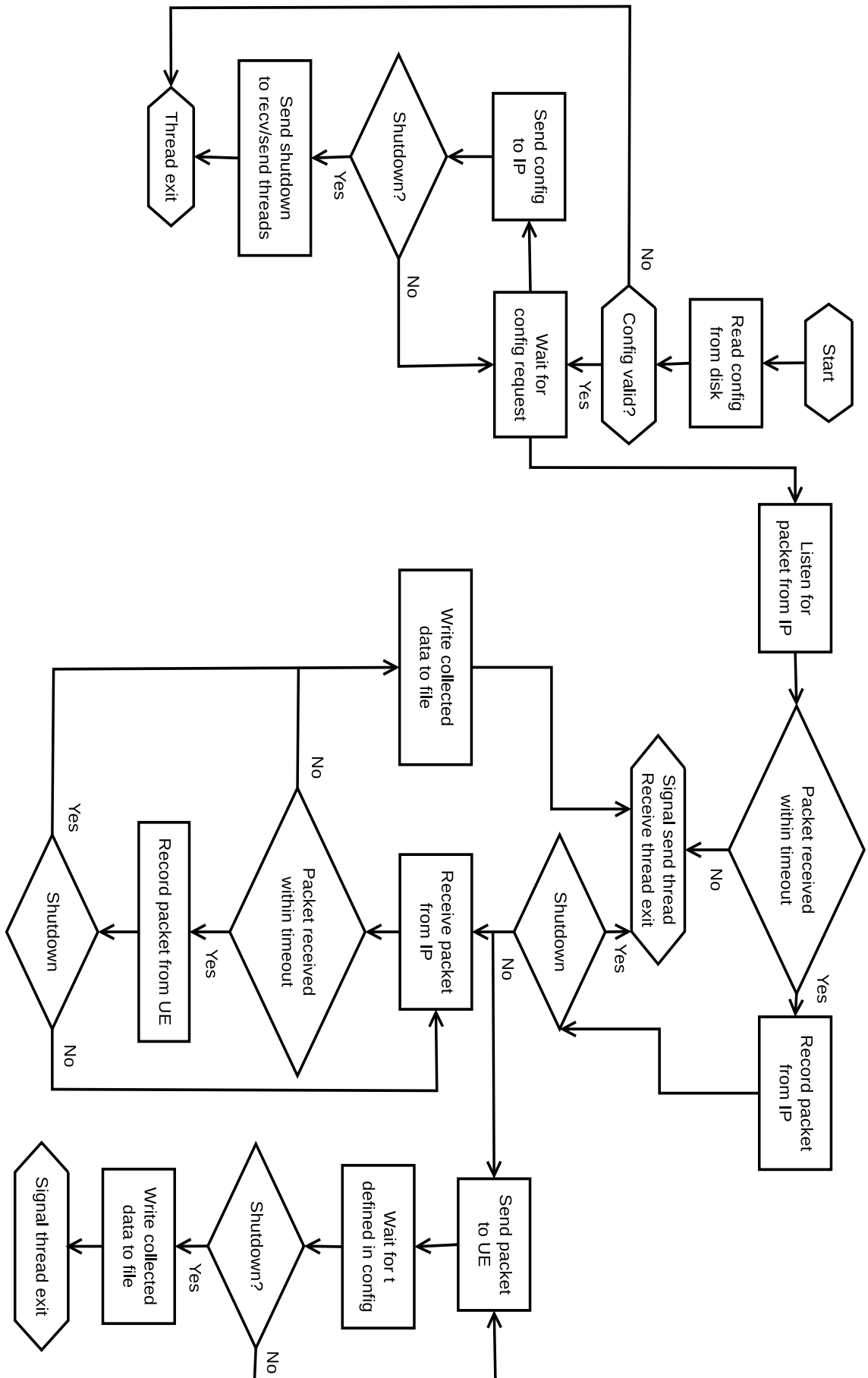


Figure 5.2 Operational diagram of server application

Apart from the server and UE client applications, an incumbent was introduced into the network. We used a cart with measurement equipment, that traveled over pre-defined path, as an incumbent. This allowed us to use it for keeping track of received interference and convey location information to the LSA system. We used R&S TSMW with log-periodic broadband antenna to measure received interference. Data from TSMW was logged to a notebook, located on the cart. Incumbent cart can be seen on Figure 5.3 in the bottom left corner.

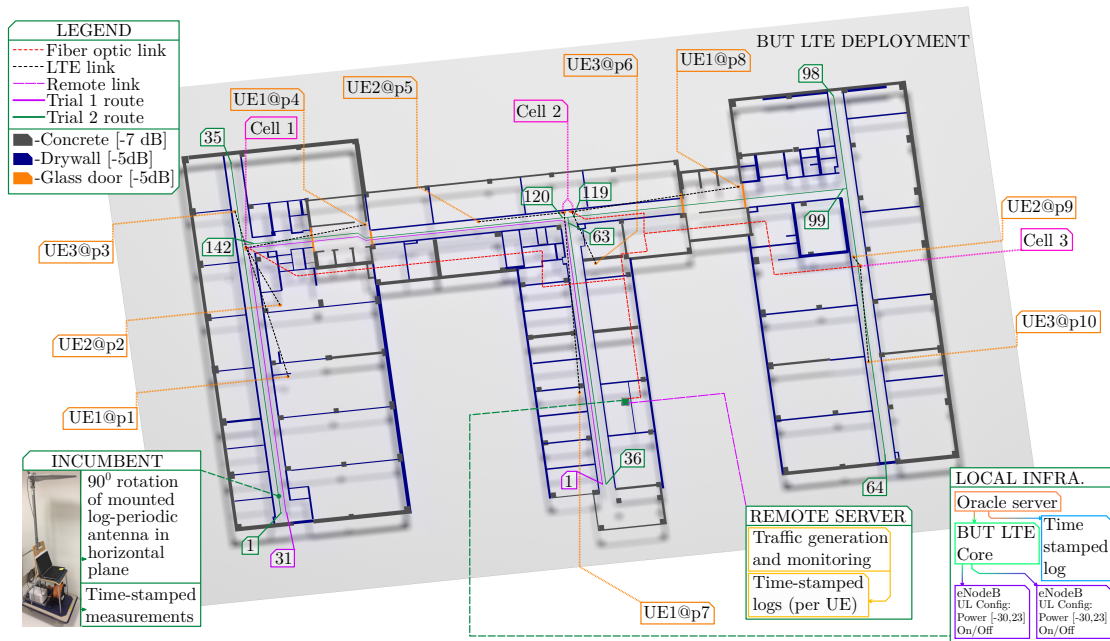


Figure 5.3 Deployment of the trial (Adapted from [3])

In order to form a coordinate system for the trial, a track with control points was made. Each of the control points was later mapped to cartesian coordinates. In Figure 5.3 measurement point indexes are defined by start and stop indexes for each segment of the path. This allowed us to make the procedure of configuring network less complex and reduce chance of erroneous input. It is also important to note that we had to devise a way to perform trial with only 4 UE devices, since we were limited in terms of hardware. In order to tackle this problem, we tested if received interference from distant UEs is low enough for us to turn them off and relocate to a new spot in the deployment. This way, when cart left first corridor (left in Figure 5.3) of the floor, all of the UE devices from it were relocated to new positions in the middle corridor. This made measurements a bit longer, but allowed us to emulate a denser scenario. Power control policies operated by connecting to the core of the network and issuing commands via configuration shell of the hardware. Special software (oracle) was written in Python for processing input data and issuing the commands to the core. In terms of LSA system, this piece of

software can be considered to be both LR and LC, while operator can be mapped to an incumbent. While first part of the statement may seem ambiguous, it can be seen that the oracle receives incumbent location and recalculates the transmit power limits based on currently configured interference limits (LR function). Furthermore, it also applies the power limits to the network (LC function). However, none of the entities represent NRA, since we initially assumed that LSA license is already obtained by licensee.

Another important difference from the simulation scenario is that we operate in an indoor environment. This introduces some differences in terms of attenuation model. Free-space path loss (FSPL) model does not apply any more, since there were almost no line-of-sight (LOS) paths between measurement cart and test UEs. In order to minimize error, we developed a small model that resembles a simplistic ray-tracer. To calculate path-loss, we define loss added by wall penetration for each material. This way we can account for walls inside the building and reduce the error. It must be noted, that despite drastically reducing the error, this approach is not fully accurate and there still were discrepancies between measurements and values predicted by our model.

Finally it is important to note that considered setup is experimental and most probably system that may emerge in 5G will differ significantly from what is described in this thesis. This is so, since 5G networks will utilize MEC to provide computationally intensive services to subscribers. These services may vary from user-oriented services, such as providing virtual machines for running computationally intensive applications on operator hardware (games, AR/VR applications) to background services used for image recognition surveillance systems [45]. This, in turn will allow network operators to both redistribute the tasks concerning power limit calculation and make the system more responsive. Latter will help network handle UE devices that are traveling at high velocities, for example phones in a moving train. Improved responsiveness comes from both increased computational power and localization of the computational tasks, thus lower delays in command loop. Moreover, operators may utilize MEC to increase maximum number of UE devices that operate on shared bands without sacrificing the responsiveness of the system compared to conventional (non-MEC) system.

5.2 Measurement results

After measurements in all of the control points were performed, we can analyze collected data. Both interference measurements and data throughput were analyzed. During the trial we measured received signal strength at the cart and configured UL TX power limits for two control methods. Plots and explanations of their behavior

are given below. Figure 5.4, which indicates limits with respect to the cart location.

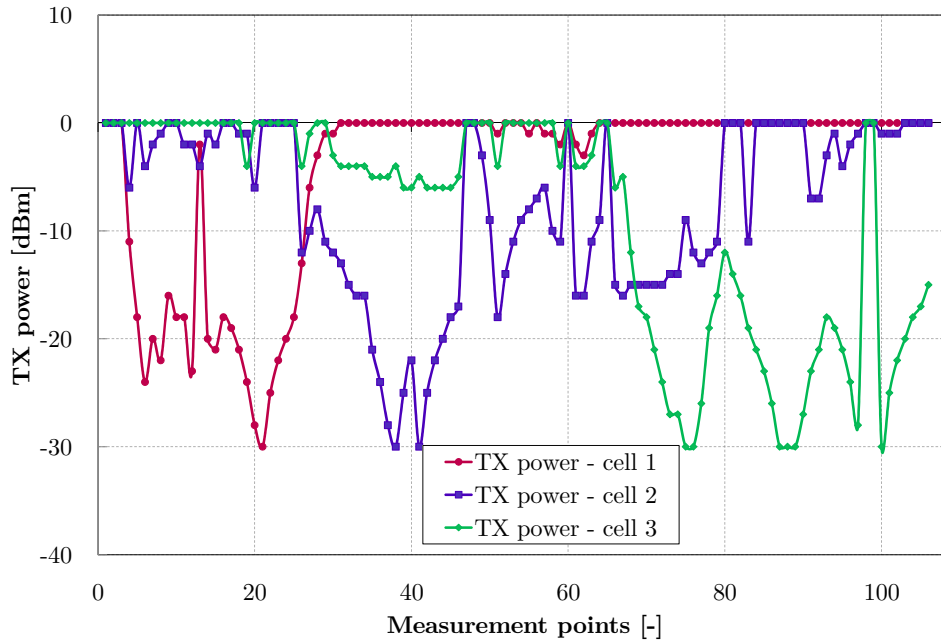


Figure 5.4 Configured UL TX power limits for SHANNON

It can be seen, that harshest limits are set when measurement cart was passing near UE devices. At certain points, when cart was in the proximity of the UE device, power control mechanism completely disabled the cell by setting UL TX power limit to values below -30 dBm. This behavior can be seen at measurement points 21 in the first corridor, when cart was near UE2 and UE3. Also, we observe similar occurrences near points 90, 100 and 75, where incumbent cart was in LOS of the licensee UE. In Figure 5.5 measured interference plot is given. A breach of the interference threshold can be seen from point 50 to 65. This breach might be explained by non-ideal propagation model. That is, in our previous studies outdoor deployments were considered. For such deployments, Okumura-Hata propagation model may be used with adjustments to scenario specifics [46, 47]. However since trial was performed in an indoor environment, we needed to devise a path-loss model to estimate interference at the incumbent cart. Our ray-based approach provided slightly more accurate results, but, as we can see, they were not always on the spot.

We also measured same characteristics for SMART LIMIT method. While it may seem that for scenario with small dimensions difference will be minuscule, we can notice them in Figure 5.6 already. They are expressed by the fact that calculated

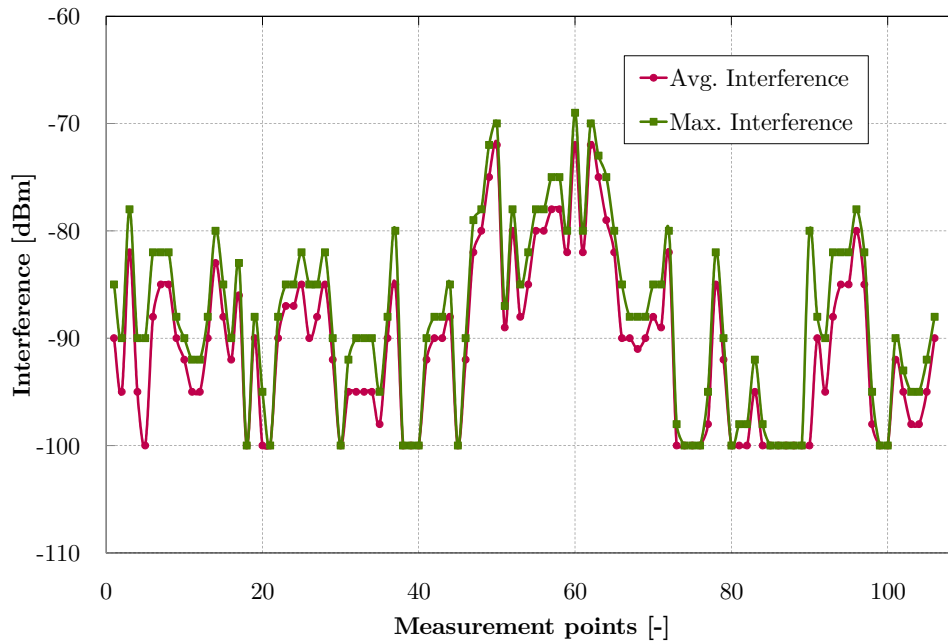


Figure 5.5 Measured interference at cart for SHANNON

limits are lower than in case of SHANNON method. This is caused by the fact that SMART LIMIT does not attempt to maintain UEs connection in operational state. Thus, it reduces UL TX limits more drastically than SHANNON. We can observe such events around point 20. SHANNON method terminated service in the network only in one instance, while SMART LIMIT reduced UL TX power below threshold at points $\{19,21\}$ and near point 30. This means that when cart is positioned near these positions, no UEs will be able to communicate with the network.

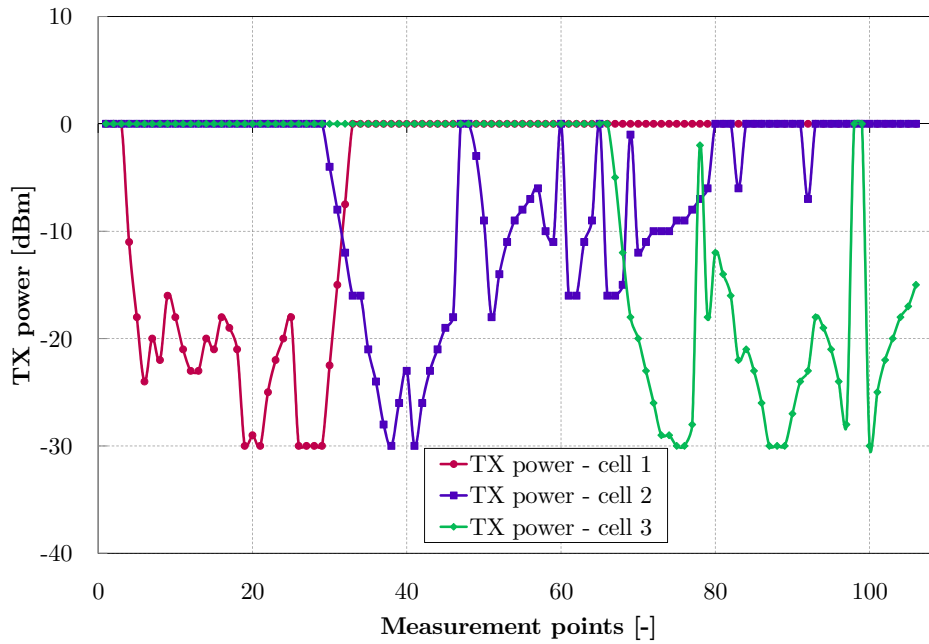


Figure 5.6 Configured UL TX power limits for SMART LIMIT

Since this method is not bound by maintenance of user connectivity, we may have expected to measure lower received interference values for SMART LIMIT. However, this effect is not that obvious from the plots in Figure 5.7.

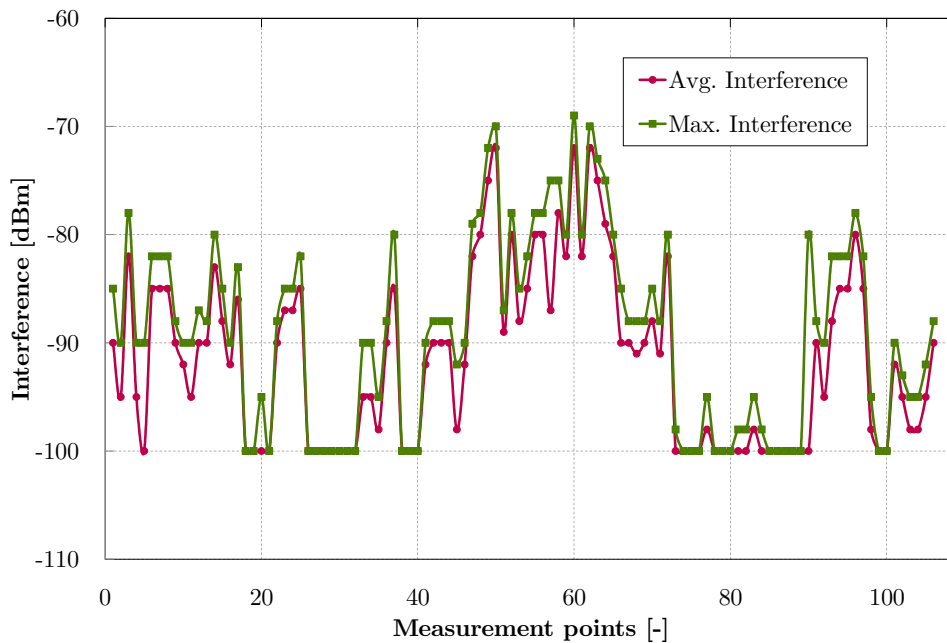


Figure 5.7 Measured interference at cart for SMART LIMIT

For example, most notable interference drops occur only near points 20 and 80, while in at other points interference values are similar to ones that were measured with SHANNON method. However, it must be noted that SHANNON method will perform more steps until satisfactory conditions are reached. Therefore, performance of the system will drop, and in case multiple users are present in the one cell, cumulative effect will take place, crippling system responsiveness. This will take place even if MEC is applied to the system, since we introduced calculation of the theoretical rate into each step.

6. CONCLUSIONS

During the study multiple options to enable dynamic operation of LSA system with incumbent were studied. All of them were non-intrusive and were designed in such way, that they will not conflict with already defined modules and entities. Instead, they will bind to already existing interfaces, and operate through them. Analytic models were compared in terms of UL TX power limit value, in order to validate the simulation results on a basic level. It was also shown in SLS results, that the simplest approach to managing interference by terminating service on shared bands in interfering cell is not the optimal solution. Numerous enhanced dynamic UL TX control methods were considered and it was shown that they can be effectively applied to interfering cells while maintaining service and adhering to the LSA license terms. A small, but rather efficient, optimization was made to the SMART LIMIT algorithm in order to decrease a number of steps needed for reaching satisfactory performance. Effect of this optimization was also studied in SLS tool. Apart from performing simulations, field trials were performed to test UL TX control methods on real LTE network. A small interference limit breach is present on the plots, that holds for all of the tested methods. Therefore, the reason of this outburst lies in the path-loss model, that was used to calculate the received signal at certain location. The model was based on simple ray-tracing for evaluating the interference at the measurement spot. Therefore, without precise information about received signal strength, it was impossible for the system to correctly calculate the penalty that must be applied to the transmit power limit in UL channel. Also, analytic methods of system performance evaluation were studied. Example of these approaches can be seen in [48, 42, 49]. To sum up all of above, it was deducted that it may be possible to satisfy the requirements of the incumbent without interrupting service on shared bands. Moreover, certain optimizations were introduced in one of the policies to reduce processing delays. However, certain challenges such as lack of precise knowledge of path-loss in indoor environments were noted. This may be mitigated in by either devising a more precise path-loss model or by using higher center frequency. It may be possible with the introduction of MEC in 5G, which will allow operators to reap benefits of having considerable amount of compute power on the edge of the network. Moreover, ray-tracing at high frequencies is a tool

widely used for estimation of channel characteristics, meaning that it may be used to produce reasonably accurate estimations of interference at the incumbent.

BIBLIOGRAPHY

- [1] “Cisco Visual Networking Index: Global Mobile Data Traffic Forecast Update 2016-2021,” tech. rep., February 7 2017. Available: <https://www.cisco.com/c/en/us/solutions/collateral/service-provider/visual-networking-index-vni/mobile-white-paper-c11-520862.pdf>.
- [2] Ericsson, “The Ericsson Mobility Report.” <https://www.ericsson.com/en/mobility-report>, 2018.
- [3] P. Mašek, E. Mokrov, K. Zeman, A. Ponomarenko-Timofeev, A. Pyattaev, S. Nesterov, S. Andreev, J. Hošek, K. Samouylov, and Y. Koucheryavy, “A Practical Perspective on 5G-Ready Highly Dynamic Spectrum Management with LSA,” *Wireless Communications and Mobile Computing*, vol. 2018, 2018.
- [4] C.-F. Lai, R.-H. Hwang, H.-C. Chao, M. M. Hassan, and A. Alamri, “A buffer-aware HTTP live streaming approach for SDN-enabled 5G wireless networks,” *IEEE Network*, vol. 29, no. 1, pp. 49–55, 2015.
- [5] E. Bastug, M. Bennis, M. Médard, and M. Debbah, “Toward interconnected virtual reality: Opportunities, challenges, and enablers,” *IEEE Communications Magazine*, vol. 55, no. 6, pp. 110–117, 2017.
- [6] M. Stusek, P. Mašek, D. Kovac, A. Ometov, J. Hošek, F. Kröpfl, and S. Andreev, “Remote management of intelligent devices: Using TR-069 protocol in IoT.,” in *Proc. of International Conference on Telecommunications and Signal Processing (TSP)*, pp. 74–78, 2016.
- [7] “Ericsson mobility report,” tech. rep., November 2018.
- [8] N. H. Mahalin, S. H. Ariffin, and R. A. Rashid, “2.4 GHz ISM band congestion: WLAN and WPAN performance analysis,” *Proc. of South East Asia Technical Universities Consortium (SEATUC)*, pp. 2–6, 2009.
- [9] A. Ometov, “Short-range communications within emerging wireless networks and architectures: A survey,” in *Proc. of 14th Conference of Open Innovations Association (FRUCT)*, pp. 83–89, IEEE, 2013.
- [10] J. van Bloem, R. Schiphorst, T. Kluwer, and C. H. Slump, “Spectrum Utilization and Congestion of IEEE 802.11 Networks in the 2.4 GHz ISM Band,” *Journal of green engineering*, vol. 2, pp. 401–430, 7 2012.

- [11] S. F. Yunas, M. Valkama, and J. Niemelä, “Spectral and energy efficiency of ultra-dense networks under different deployment strategies,” *IEEE Communications Magazine*, vol. 53, no. 1, pp. 90–100, 2015.
- [12] A. Gotsis, S. Stefanatos, and A. Alexiou, “UltraDense networks: The new wireless frontier for enabling 5G access,” *IEEE Vehicular Technology Magazine*, vol. 11, no. 2, pp. 71–78, 2016.
- [13] E. Yaacoub and M. Al-Husseini, “Achieving physical layer security with massive MIMO beamforming,” in *Proc. of 11th European Conference on Antennas and Propagation (EUCAP)*, pp. 1753–1757, March 2017.
- [14] A. Mukherjee and A. Swindlehurst, “Robust Beamforming for Security in MIMO Wiretap Channels With Imperfect CSI,” *IEEE Transactions on Signal Processing*, vol. 59, pp. 351–361, Jan 2011.
- [15] Z. Gao, L. Dai, D. Mi, Z. Wang, M. A. Imran, and M. Z. Shakir, “mmWave massive-MIMO-based wireless backhaul for the 5G ultra-dense network,” *IEEE Wireless Communications*, vol. 22, no. 5, pp. 13–21, 2015.
- [16] M. K. Samimi, S. Sun, and T. S. Rappaport, “MIMO channel modeling and capacity analysis for 5G millimeter-wave wireless systems,” in *Proc. of 10th European Conference on Antennas and Propagation (EuCAP)*, pp. 1–5, IEEE, 2016.
- [17] F. W. Vook, A. Ghosh, and T. A. Thomas, “MIMO and beamforming solutions for 5G technology,” in *Proc. of MTT-S International Microwave Symposium (IMS)*, pp. 1–4, IEEE, 2014.
- [18] B. Van der Bergh, A. Chiumento, and S. Pollin, “LTE in the sky: trading off propagation benefits with interference costs for aerial nodes,” *IEEE Communications Magazine*, vol. 54, no. 5, pp. 44–50, 2016.
- [19] R. Kovalchukov, D. Moltchanov, A. Samuylov, A. Ometov, S. Andreev, Y. Koucheryavy, and K. Samouylov, “Analyzing Effects of Directionality and Random Heights in Drone-Based mmWave Communication,” *IEEE Transactions on Vehicular Technology*, vol. 67, no. 10, pp. 10064–10069, 2018.
- [20] J. Pokorny, A. Ometov, P. Pascual, C. Baquero, P. Masek, A. Pyattaev, A. Garcia, C. Castillo, S. Andreev, J. Hošek, *et al.*, “Concept design and performance evaluation of UAV-based backhaul link with antenna steering,” *Journal of Communications and Networks*, vol. 20, no. 5, pp. 473–483, 2018.

- [21] A. Ometov, E. Olshannikova, P. Mašek, T. Olsson, J. Hošek, S. Andreev, and Y. Koucheryavy, “Dynamic trust associations over socially-aware D2D technology: A practical implementation perspective,” *IEEE Access*, vol. 4, pp. 7692–7702, 2016.
- [22] M. Belleschi, G. Fodor, and A. Abrardo, “Performance analysis of a distributed resource allocation scheme for D2D communications,” in *Proc. of GLOBECOM Workshops (GC Wkshps)*, pp. 358–362, IEEE, 2011.
- [23] S. Andreev, D. Moltchanov, O. Galinina, A. Pyattaev, A. Ometov, and Y. Koucheryavy, “Network-assisted device-to-device connectivity: contemporary vision and open challenges,” in *Proc. of 21th European Wireless Conference*, pp. 1–8, VDE, 2015.
- [24] M. Matinmikko, H. Okkonen, M. Palola, S. Yrjola, P. Ahokangas, and M. Mustonen, “Spectrum sharing using licensed shared access: the concept and its workflow for LTE-advanced networks,” *IEEE Wireless Communications*, vol. 21, no. 2, pp. 72–79, 2014.
- [25] Z. Sadreddini, P. Masek, T. Cavdar, A. Ometov, J. Hosek, I. Gudkova, and S. Andreev, “Dynamic Resource Sharing in 5G with LSA: Criteria-Based Management Framework,” *Wireless Communications and Mobile Computing*, 2018.
- [26] E. Markova, I. Gudkova, A. Ometov, I. Dzantiev, S. Andreev, Y. Koucheryavy, and K. Samouylov, “Flexible Spectrum Management in a Smart City within Licensed Shared Access Framework,” *IEEE Access*, vol. 5, pp. 22252–22261, 2017.
- [27] A. Haidine and S. El Hassani, “LTE-a pro (4.5 G) as pre-phase for 5G deployment: closing the gap between technical requirements and network performance,” in *Proc. of International Conference on Advanced Communication Systems and Information Security (ACOSIS)*, pp. 1–7, IEEE, 2016.
- [28] M. Palola, M. Matinmikko, J. Prokkola, M. Mustonen, M. Heikkilä, T. Kippola, S. Yrjölä, V. Hartikainen, L. Tudose, A. Kivinen, J. Paavola, K. Heiska, T. Hänninen, and J. Okkonen, “Description of finnish Licensed Shared Access (LSA) field trial using TD-LTE in 2.3 GHz band,” in *Proc. of IEEE International Symposium on Dynamic Spectrum Access Networks (DYSPAN)*, pp. 374–375, April 2014.
- [29] M. Palolo, T. Rautio, M. Matinmikko, J. Prokkola, M. Mustonen, M. Heikkilä, T. Kippola, S. Yrjölä, V. Hartikainen, L. Tudose, A. Kivinen, J. Paavola, J. Okkonen, M. Mäkeläinen, T. Hänninen, and H. Kokkinen, “Licensed Shared

- Access (LSA) trial demonstration using real LTE network,” in *Proc. of 9th International Conference on Cognitive Radio Oriented Wireless Networks and Communications (CROWNCOM)*, pp. 498–502, June 2014.
- [30] “ECC Report 172: Broadband Wireless Systems Usage in 2300-2400 MHz,” tech. rep., Mar 2012.
- [31] P. Mašek, E. Mokrov, A. Pyattaev, K. Zeman, A. Ponomarenko-Timofeev, A. Samuylov, E. Sopin, J. Hošek, I. A. Gudkova, S. Andreev, *et al.*, “Experimental evaluation of dynamic Licensed Shared Access operation in live 3GPP LTE system,” in *Proc. of Global Communications Conference (GLOBECOM)*, pp. 1–6, IEEE, 2016.
- [32] “FM52(15)13: LSA Demonstration carried out in the Mobile World Congress, Barcelona,” tech. rep., May 2015.
- [33] “System architecture and high level procedures for operation of Licensed Shared Access (LSA) in the 2 300 MHz – 2 400 MHz band,” tech. rep., October 2015. Available: http://www.etsi.org/deliver/etsi_ts/103200_103299/103235/01.01.01_60/ts_103235v010101p.pdf.
- [34] “Mobile broadband services in the 2300 MHz - 2400 MHz frequency band under Licensed Shared Access regime,” tech. rep., July 2017. Available: http://www.etsi.org/deliver/etsi_tr/103100_103199/103113/01.01.01_60/tr_103113v010101p.pdf.
- [35] “RSPG Opinion on Licensed Shared Access,” tech. rep., 2013.
- [36] E. Mohyeldin, “LSA facilitates national spectrum access to globally harmonized IMT spectrum,” tech. rep., 2013.
- [37] A. Pyattaev, “Winter SLS Distribution,” March 2014. Available: <http://winter-group.net/download/>.
- [38] E. Jones and T. Oliphant and P. Peterson and others, “SciPy: Open source scientific tools for Python.” <http://www.scipy.org/>, 2001–2018. [Online; accessed Dec. 2018].
- [39] B. Christiansen and M. Garey and I. Hartung, “Slurm Overview,” tech. rep., 2017.
- [40] “About GlusterFS,” tech. rep., 2017.

- [41] V. Borodakiy, K. Samouylov, I. Gudkova, D. Ostriкова, A. Ponomarenko-Timofeev, A. Turlikov, and S. Andreev, “Modeling unreliable LSA operation in 3GPP LTE cellular networks,” pp. 390–396, 2014.
- [42] I. Gudkova, K. Samouylov, D. Ostriкова, E. Mokrov, A. Ponomarenko-Timofeev, S. Andreev, and Y. Koucheryavy, “Service failure and interruption probability analysis for Licensed Shared Access regulatory framework,” in *Proc. of 7th International Congress on Ultra Modern Telecommunications and Control Systems and Workshops (ICUMT)*, pp. 123–131, Oct 2015.
- [43] “ETSI White Paper No. 28: MEC in 5G networks,” tech. rep., June 2018.
- [44] “5G: A Technology Vision,” tech. rep., 2013.
- [45] “ETSI White Paper No. 30: MEC in an Enterprise Setting: A Solution Outline,” tech. rep., September 2018.
- [46] N. Elfadhil, M. A. Salam, A. Al-Lawati, O. Al-Qasmi, M. Al-Gheithi, and Z. Nadir, “Modification of an Open Area Okumura-Hata Propagation Model Suitable for Oman,” in *Proc. of TENCON 2005*, pp. 1–4, Nov 2005.
- [47] A. Medeisis and A. Kajackas, “On the use of the universal Okumura-Hata propagation prediction model in rural areas,” in *Proc. of 51st Vehicular Technology Conference Proceedings (Cat. No.00CH37026)*, vol. 3, pp. 1815–1818, 2000.
- [48] M. E.V., P.-T. A.A., I. Gudkova, S. Andreev, and K. Samouylov, “Modeling a load balancing scheme between primary licensed and LSA frequency bands,” in *Proc. of IX International Workshop “Applied Problems in Theory of Probabilities and Mathematical Statistics related to modeling of information systems” APTP+MS-2015*, 08 2015.
- [49] E. Mokrov, A. Ponomarenko-Timofeev, I. Gudkova, P. Mašek, J. Hošek, S. Andreev, Y. Koucheryavy, and Y. Gaidamaka, “Modeling Transmit Power Reduction for a Typical Cell with Licensed Shared Access Capabilities,” *IEEE Transactions on Vehicular Technology*, vol. 67, no. 6, p. 5505, 2018.